KTH Industrial Engineering
and Management

INFRARED EMITTANCE OF PAPER
– METHOD DEVELOPMENT, MEASUREMENTS AND APPLICATION

Caroline Hyll

Licentiate Thesis

School of Industrial Engineering and Management
Department of Production Engineering
The Royal Institute of Technology, Stockholm
NOVEMBER 2012

TRITA-IIP-12-10
ISSN 1650-1888

Department of Production Engineering
The Royal Institute of Technology
SE-100 44 Stockholm

Abstract

Thermography is a non-destructive technique which uses infrared radiation to obtain the temperature distribution of an object. The technique is increasingly used in the pulp and paper industry. To convert the detected infrared radiation to a temperature, the emittance of the material must be known. For several influencing parameters the emittance of paper and board has not previously been studied in detail. This is partly due to the lack of emittance measurement methods that allow for studying the influence of these parameters.

An angle-resolved goniometric method for measuring the infrared emittance of a material was developed in this thesis. The method is based on the reference emitter methodology, and uses commercial infrared cameras to determine the emittance. The method was applied to study the dependence on wavelength range, temperature, observation angle, moisture ratio, sample composition, and sample structure of the emittance of paper and board samples. It was found that the emittance varied significantly with wavelength range, observation angle and moisture ratio. The emittance was significantly higher in the LWIR (Long-Wavelength Infrared) range than in the MWIR (Mid-Wavelength Infrared) range. The emittance was approximately constant up to an observation angle of 60° in the MWIR range and 70° in the LWIR range, respectively. After that it started to decrease. The emittance of moist samples was significantly higher than that of dry samples. The influence of moisture ratio on the emittance could be estimated based on the moisture ratio of the sample, and the emittance of pure water and dry material, respectively.

The applicability of measured emittance values was demonstrated in an investigation of the mechanical properties of sack paper samples. An infrared camera was applied to monitor the generation of heat during a tensile test of a paper sample. It was found that the observed increase in thermal energy at the time of rupture corresponded well to the value of the elastic energy stored in the sample just prior to rupture. The measured emittance value provided an increased accuracy in the thermal energy calculation based on the infrared images.

Keywords: Emittance, Emissivity, Thermography, Paper, Sheet, Papermaking, Paper mechanics, Moisture, Material properties, Reflectance, Transmittance, Absorptance, Infrared, Mid-wavelength infrared, MWIR, Long-wavelength infrared, LWIR, Angle-resolved, Directional.

Acknowledgments

I owe great thanks to my supervisors, Dr. Hannes Vomhoff at Innventia and Prof. Lars Mattsson at KTH Royal Institute of Technology. Hannes Vomhoff has provided seemingly unwavering energy, enthusiasm and belief in my abilities. Lars Mattsson has offered a calm and warm space at the Department of Production Engineering, with thoughtful feedback and scientific discussions. Furthermore, I am deeply grateful to Prof. Bo Norman for his feedback when writing this thesis.

I have been lucky to share my room. First, Rasmus Andersson provided guidance and inspiration. Then Aron Tysén inherited his desk and provided the best possible support, feedback and discussion on scientific and non-scientific things. Also at Innventia, I would like to thank the Paper Technology group for their constant support. Fredrik Rosén, while no longer part of the group, also owes my thanks for his friendly and enthusiastic guidance. The Paper Mechanics group has given me knowledge and insight into a new field. In the Optics and Metrology group at the Department of Production Engineering, Rong Su has always provided quick and friendly help in small and large issues.

This work would not have been possible without the technical and experimental support of many people; Claes Öhman, Prof. Arne Roos, Sune Karlsson, the Pulp Characterization lab crew at Innventia, and many others.

It is not a clear-cut path for an astronomer to start working with paper. But the knowledge and skills of light and radiation, detection and analysis acquired during my Master's education have proved invaluable. I would therefore like to send thanks to the Astronomy Department at Stockholm University. Also, thanks to the people at Savantic, for planting the seed of this path.

Finally, I would like to thank my family, friends and acquaintances – those of you who have pursued this path before me and provided inspiration and hope, and those of you who have provided creativity, joy and love during this time. And Björn Thenstedt, thanks for being there.

"Every student who enters upon a scientific pursuit, especially if at a somewhat advanced period of life, will find not only that he has much to learn, but much also to unlearn."

- *Sir William Herschel*
Astronomer and discoverer of the infrared

Table of contents

1 Introduction

1.1 Background

Thermography is a non-destructive technique which uses the emitted infrared radiation to determine the surface temperature distribution of an object. The technique is increasingly used in the pulp and paper industry. To convert the detected infrared radiation to temperature, the emittance of the material must be known. The emittance is a radiative material property which may vary with wavelength, temperature, observation angle, moisture content, material composition, material structure, and surface roughness. An as exact as possible emittance value for a given measurement situation is therefore crucial for the accuracy of thermographic measurements.

1.2 Problem statement

The emittance of paper has not been studied for many of the conditions that are encountered in a paper mill. This general lack of information may partly be explained by limitations of existing emittance measurement methods. No emittance measurement method that allows for variation of temperature, observation angle and moisture ratio exist. Additionally, the emittance of paper may not be predicted by current analytical models. The limitations of existing models stress the importance of measuring the emittance.

1.3 Objective

The aim of this thesis is to improve the accuracy of thermographic measurements in the pulp and paper industry by providing emittance values for different materials under different process conditions. These values can also be used in future modelling of infrared emission from paper at different stages in the papermaking process.

1.4 Methodology

Based on a thorough literature study providing state of the art knowledge, a new angle-resolved goniometric emittance measurement method suitable for paper samples exposed to different temperatures and moisture ratios was developed. Followed by verification testing and error analysis of the system, a large number of angle-resolved emittance measurements were made on paper and board under conditions similar to those at different stages in the papermaking process. The applicability of measured emittance values to quantitative thermographic measurements was demonstrated.

1.5 Overview

This thesis is organized in five chapters. Chapter 1 comprises this introduction. In Chapter 2, theory and background on thermography, emittance and papermaking are given. Here, an introduction to the interaction between electromagnetic radiation and a material is provided. Available theories for predicting the behaviour of the emittance are discussed,

and radiative material properties that are complementary to the emittance are introduced. Different methods for measuring the emittance are reviewed. An overview on papermaking is given and problems related to temperature and moisture variations are discussed. The use of thermography within the pulp and paper industry is reviewed. Chapter 3 presents the experimental part of this thesis. The development of an angle-resolved goniometric method for emittance measurements is described. Then, the method is applied to measure the emittance of dry and moist paper and board. Emittance measurement results are applied in an investigation on the rupture of paper. The results from the experimental work are presented and discussed in Chapter 4. In Chapter 5, the main results of this work are summarized and suggestions for future work are given.

2 Theory and background

2.1 Thermography and emittance

Thermography is a technique that can be used for non-destructive inspection, evaluation and testing of materials and processes. Most commonly, it is used to obtain a temperature image of an object's surface. In a very common application, thermography is used to examine buildings for badly isolated windows or interior moisture damage. *Figure 2.1* shows a comparison of a visual and an infrared image of a moisture-damaged building, where evaporative cooling by water desorption decreases the temperature of the wall.

Figure 2.1. Visual (left) and infrared (right) image of a house with a water-leaking washing machine on the third floor. Adapted from Philips [1].

Thermography operates on the principle that all objects with a temperature above zero Kelvin emit radiation. At material temperatures up to a few hundred degrees Celcius, most of the radiation is emitted in the infrared range [2]. The infrared range of the electromagnetic spectrum is loosely defined as the wavelengths between 0.8 and 1000 µm. Commonly, two wavelength ranges, known as the Mid-Wavelength Infrared ("MWIR", approximately 3-5 µm) and the Long-Wavelength Infrared ("LWIR", approximately 8-15 µm) are used in thermography. Detection outside of these ranges is limited due to sensor material properties and atmospheric absorption.

In thermography, infrared detectors are used to measure the radiation emitted by objects due to their temperature [3, 4]. Previously, point-like sensors were used. Today, thermography usually refers to the use of 2D sensors giving temperature images, i.e. infrared cameras. For most infrared cameras, the emitted radiance incident on the detector will create a signal voltage U that is proportional to the radiance. The camera may convert the signal voltage to a temperature measurement using Planck's law. For any wavelength λ in the electromagnetic spectrum, Planck's law relates the emitted spectral

radiance $L_{bb\lambda}$ of a true blackbody to the absolute temperature T measured in K of the emitting object. For a small wavelength interval $d\lambda$ around λ, it is expressed as:

$$L_{bb\lambda}d\lambda = \frac{2hc^2}{\lambda^5(e^{hc/\lambda kT} - 1)}d\lambda \qquad \text{(eq. 2.1)}$$

where h is Planck's constant, c is the speed of light in vacuum, λ is the wavelength at which the radiation is emitted, and k is Boltzmann's constant. Most materials only emit a fraction of the radiation that a blackbody would emit under identical conditions. This fraction, the emissivity ε, is a thermal radiative material property unique to each material. For an object emitting the spectral radiance $L_{obj\lambda}$, the emissivity is defined as:

$$\varepsilon = \frac{L_{obj\lambda}}{L_{bb\lambda}} \qquad \text{(eq. 2.2)}$$

where $L_{bb\lambda}$ is the emitted spectral radiance from a true blackbody under the same conditions. In thermographic literature, emissivity and emittance are often used interchangeably. However, efforts have been made to distinguish the ideal property (emissivity) from the measured property (emittance) [5, 6]. In this work, emissivity is reserved for the theoretical sections while the word emittance is used for the same property, when measurements on real materials with a limited thickness are discussed.

According to *eq. 2.2,* the emittance ε relates the emitted spectral radiance $L_{obj\lambda}$ from an object to the corresponding spectral radiance of a blackbody, $L_{bb\lambda}$, which can be used to obtain a temperature by solving *eq. 2.1*. However, infrared cameras cannot automatically detect the emittance. If the emittance is not provided, the camera commonly calculates a temperature based on a default emittance value. Thus, the calculated temperature may deviate significantly from the true temperature of the material [7]. While thermography is also influenced by factors such as the temperature of the surroundings reflected by the measured object, and the humidity of the air, the emittance is the single greatest error source in thermography [8].

2.2 Interaction between infrared radiation and a material

Thermography is based on emitted infrared radiation. For a molecular material, the emission is usually caused by thermal excitation of vibrations and rotations of molecules due to the temperature of the material. This temperature can be received by conduction of heat, convection through warm air, or by absorbed electromagnetic radiation that turns into heat and re-irradiates as infrared radiation. Thus, the emittance of a material is closely linked to the material's ability to absorb incident radiation. Radiation incident on a surface may not only be absorbed, but also be reflected and/or transmitted. *Figure 2.2* illustrates reflection, transmission, absorption and emission of radiation in the ideal case of a super-smooth, homogeneous material:

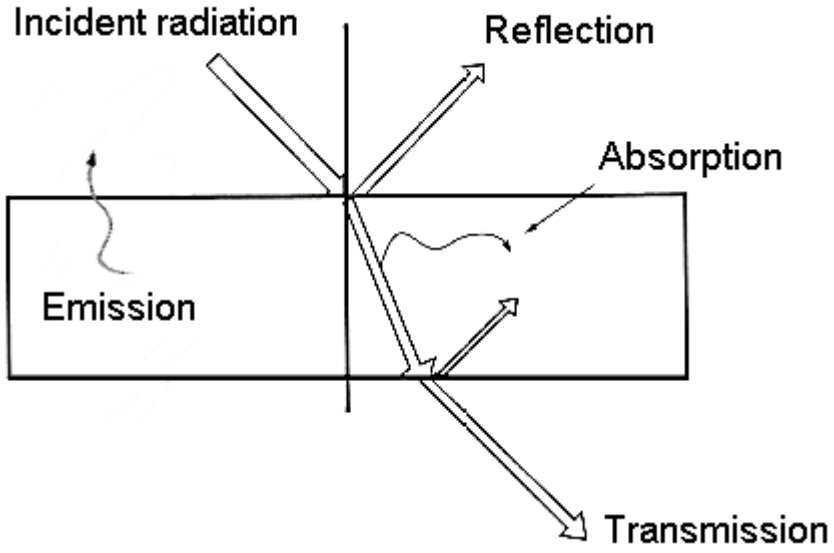

Figure 2.2. Reflection, transmission, absorption and emission of radiation in the ideal case of a super-smooth, homogeneous material, for example visual light incident on a colored piece of glass.

When radiation is reflected at a super-smooth flat surface, a mirror-like, specular reflection occurs, where the wave front of the radiation is preserved, and thereby the relation between the angle of incidence and angle of reflection. If the surface is instead rough, the radiation is diffusely reflected and re-distributed in space (scattered). Generally, a high surface roughness, i.e. when the wavelength of the radiation is small compared to the typical size of the surface structures, corresponds to a high scattering of both the reflected and transmitted radiation.

Most materials have a mixture of specular and diffuse reflective qualities. In an inhomogeneous material such as paper, the geometry of the surface may vary significantly dependent on the distribution and orientation of the fibres and additives. Thus, facets at the surface of a paper sheet may be flat or curved, and smooth or rough. An example is given *Figure 2.3*, where a microscopic image of the surface of a low grammage paper sheet is presented.

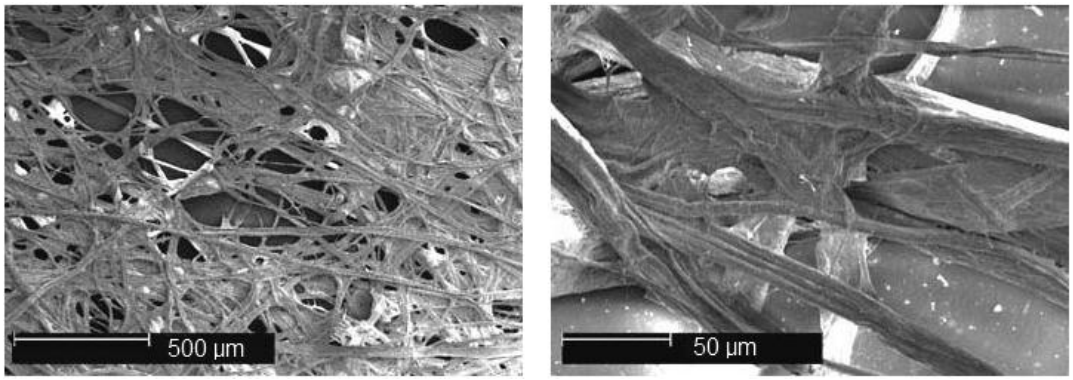

Figure 2.3. Paper for teabags, viewed under a microscope with low (left) and high (right) magnification [9].

When both the surface and volume (interior) of a material is inhomogeneous, as in the case of paper, the interaction between incident radiation and the material is complex. Here, scattering re-distributes the radiation into many directions as it propagates through the material. While some of the radiation is scattered through the material (i.e. transmitted), some of it is absorbed and turned into heat before it can exit the material as thermal infrared radiation. *Figure 2.4* illustrates different interactions between radiation and the surface and volume of a paper sheet.

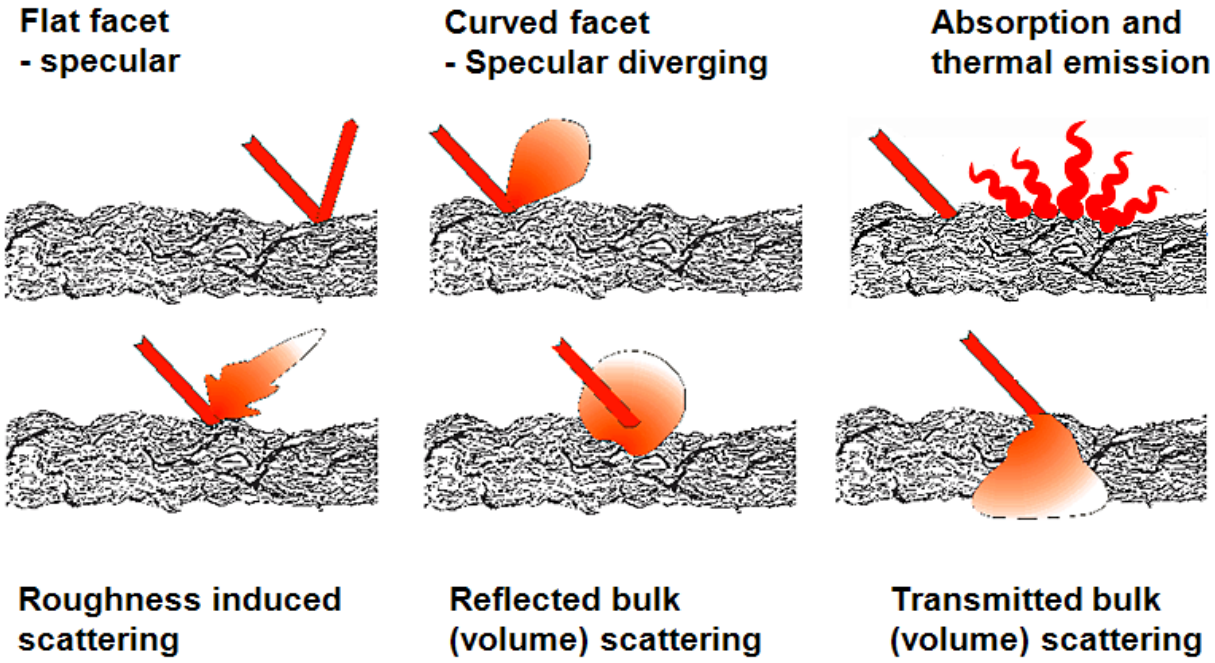

Figure 2.4. Illustration of interactions between radiation and the surface and volume of a paper sheet [10].

Since the emittance of a material is defined by its emissive capacity *(eq. 2.2)*, and emission is linked to the propagation of radiation in the material, understanding the emittance require understanding of the fundamental interactions between radiation and a material. There is no unified theory for predicting the interaction between radiation and a material. Instead, different theories are used dependent on the size of the structures in the material and the wavelength of the radiation. When the wavelength of the radiation is small compared to the geometrical structures in the material, geometrical optics can be used to describe the interaction, and Monte-Carlo simulations can be used to model the

interaction with rather complex structures [11]. In geometrical optics, the complex refractive index *n* of the material plays a significant role, in the sense that the reflectance at an interface is large if the difference in refractive index of the two media is large [12].

For example, if geometrical optics is used to predict the interaction between visible light and moist paper, air/water, air/fibre and water/fibre interfaces must be considered. Here, the refractive index of air (n = 1.00) is lower than the refractive index of water (n = 1.33), which in turn is lower than the refractive index of wooden fibres (n = 1.55) [13-15]. Thus, the difference in refractive index is larger for an air/fibre interface than for an air/water interface. This explains why wet paper gets more transparent at visible wavelengths, as pores between the fibres and within the fibre wall fills with water, and replace fibre/air interfaces. Consequently, scattering due to reflections decreases and the paper becomes more transparent. Additionally, if the fibre network is compressed, more fibres will be in direct contact with each other and the number of air or water pores will decrease. This reduces the number of air/fibre interfaces, and thereby the scattering. Thus, a calendering process, that compresses the fibre network irreversibly, makes the paper more transparent.

When considering the interaction between paper and infrared radiation at typical thermographic wavelengths, radiation with wavelengths between 3 and 15 μm interacts with structures that are typically 3 to 50 μm (see *Figure 2.3*). Thus, the wavelength of the radiation may be of the same order of magnitude as the physical structures in a paper sheet. Here, geometrical optics is a poor predictor of the interaction, which may explain why no published values on the refractive index of paper at typical thermographic wavelengths were found. Instead of geometrical optics, the scattering theory of Mie may be used in this regime [16]. However, the Mie theory assumes spherical particles that are not too closely packed. The inhomogeneous size and structure of the fibre network in paper limits the usefulness of the Mie scattering theory for predicting the propagation of radiation in paper. Due to the limitations of analytical models, semi-empirical models or conceptual descriptions are commonly used for predicting for the propagation of infrared radiation in paper [17].

The most widely investigated semi-empirical model in describing the interaction between radiation and paper is the Kubelka-Munk theory of reflectance. The Kubelka-Munk theory was developed for the study of layers of paints in visible light. [18]. A few studies have used the Kubelka-Munk theory to predict the emittance of a material [19, 20]. However, no report was found where the Kubelka-Munk theory was used to predict the interaction between paper and infrared radiation in general or the emittance of paper in particular. A possible explanation is the reported limitations of the Kubelka-Munk theory when it is applied to highly absorptive materials, such as paper in the infrared range [18]. In a recent study, a model related to the Kubelka-Munk theory [21] was evaluated by transmission and reflection measurements of ceramics, in the near-infrared wavelength range [22]. The model was valid for both low-scattering (i.e. highly absorptive) and high-scattering samples, making it an interesting candidate for future modelling of the interaction between radiation and paper in the infrared range.

Theoretical models of the interaction between radiation and a material can be tested and refined by comparison with measurements that quantify the interaction. In the case of infrared radiation and paper, the limitations of existing models stress the importance of

measurements to gain fundamental understanding of this interaction. Examples of such measurable quantities, here referred to as radiative material properties, are the transmittance, reflectance, absorptance and emittance.

For a given material and incident wavelength, the transmittance τ is defined as the ratio of transmitted radiation relative to incident radiation, see *Figure 2.2*. Correspondingly, the absorptance α is the ratio of absorbed radiation relative to incident radiation, and the reflectance ρ is the ratio of reflected radiation relative to incident radiation. Emittance, reflectance, transmittance and absorptance are dimensionless quantities. Their values range from 0 to 1, dependent on many parameters, for example temperature, wavelength, observation angle, material composition, material structure, and surface roughness. Due to conservation of energy, the sum of reflectance, transmittance and absorptance, under steady-state conditions, must equal one [2, 3, 6]:

$$\rho + \tau + \alpha = 1 \qquad \text{(eq. 2.3)}$$

According to Kirchoff's law, under steady-state conditions, all absorbed radiation at a given wavelength and incidence/observation angle must be re-emitted [2, 3]:

$$\alpha = \varepsilon \qquad \text{(eq. 2.4)}$$

Hence, when reviewing literature sources in this work, measurements results for the absorptance were assumed to correspond to the emittance of the material in question. *Eq. 2.3* then becomes

$$\rho + \tau + \varepsilon = 1 \qquad \text{(eq. 2.5)}$$

For opaque materials, i.e. $\tau = 0$, *eq. 2.5* can be written as:

$$\varepsilon = 1 - \rho \qquad \text{(eq. 2.6)}$$

This relationship between emittance and reflectance is often used to derive emittance values based on reflectance measurements [23].

Using a defined nomenclature is helpful when describing the measurement method [3]. When measured at a specific observation angle (usually normal to the surface), these properties are called "directional" (e.g. directional emittance). When the measurement is integrated over all possible directions in the hemisphere above the radiating material, the property is called "hemispherical". A property that is measured at a specific wavelength is called "spectral" (e.g. spectral emittance). When measured over a specific wavelength band (e.g. the MWIR range) the property is called "integrated", while a measurement that is integrated over the entire spectrum is commonly called "total". Values of emittance given in literature tables are often total hemispherical or total normal. In most thermographic measurement situations, using an emittance that is directional (given for the present observation angle) and integrated (over the wavelength sensitivity of the camera sensor) will improve the accuracy of the temperature measurement.

Methods for measuring emittance comprise standardized (e.g. [24, 25]), and non-standardized methods and equipment (e.g. [23, 26-29]). Most experimental work on the

determination of the emittance of paper used non-standardized methods [29-32]. Non-standardized methods include reflectivity methods, reference emitter methods and reference temperature methods. The methods may either measure directional emittance or hemispherical emittance.

Reflectivity methods determine emittance indirectly by measuring the reflectance and transmittance of the material, using *eq. 2.5* to determine the emittance. Most reflectance and transmittance measurements are performed with Fourier Transform Infrared spectroscopy (FTIR), which usually measures the hemispherical emittance [33, 34].

Reference emitter methods determine emittance by comparing the radiation of the material to that of a reference surface under identical conditions. Here, the emittance of the reference needs to be known [6]. Reference temperature methods determine the emittance of a material under the requirement that the temperature of the material is well known. Reference emitter and reference temperature methods require the sample to be opaque (have a transmittance of zero) in the wavelength sensitivity range of the sensor, but can be carried out with normal infrared cameras. Furthermore, the sample should be heated to temperatures above ambient temperature in order to achieve sufficient signal contrast between the samples and the environment [6].

The limitations of existing theories and methods to predict and measure the emittance of a material in general, and paper in particular, have been addressed in this section. The measurement of paper emittance values will both improve the accuracy of future thermographic measurements in the pulp and paper industry, and provide a basis for future modelling of infrared emission from paper at different stages in the papermaking process. As mentioned before, several parameters influence the emittance of a material. In order to determine which factors influence the emittance of paper, an understanding into the papermaking process is needed. Here, results already achieved by thermography in the pulp and paper industry can be of assistance.

2.3 Use of thermography in paper production

The main component of paper is fibres derived from wood, a major natural resource in Sweden. The pulp and paper industry is one the country's base industries; in 2011 employing over 20 000 persons and accounting for an export of about 70 billion SEK [35]. Its annual energy consumption of 20 TWh (2011) makes the pulp and paper industry one of the most energy consuming industries in Sweden. During recent decades the industry has seen a significant reduction in specific energy use due to improved production processes. However, development of new processes and technologies are still necessary to meet the ever-increasing requirement of energy efficiency. One potential area for energy savings is an improvement of the efficiency of the production process and reducing the variability in the final products.

Industrial papermaking can be considered as a technically advanced high-speed production process (600 to 2000 m/min) where water is removed from a pulp suspension, leaving a web consisting mainly of fibres and some additives. The pulp may be composed of several fibre types, for example softwood (e.g. pine, spruce) or hardwood (e.g. birch, eucalyptus) fibres. Different processes are used to extract the fibres from the wooden raw material. For example, the chemical process removes most of the lignin that binds the fibres together, resulting in individually separated fibres, while the thermo-mechanical process disintegrates the wood by mechanical force. Thermo-mechanical pulp (TMP) usually has a higher content of fine material, fibre fragments, and lignin. The pulp may then be bleached for an additional removal of lignin and increased brightness.

In the first section of a paper machine, a headbox delivers the pulp suspension onto a supportive, permeable forming wire. Different pulps may be delivered in several plies, for example in a board product, in order to control product properties in the thickness direction. *Figure 2.5* illustrates a single layer paper sheet and a multi-ply board sheet, together with definitions of the different directions in a sheet.

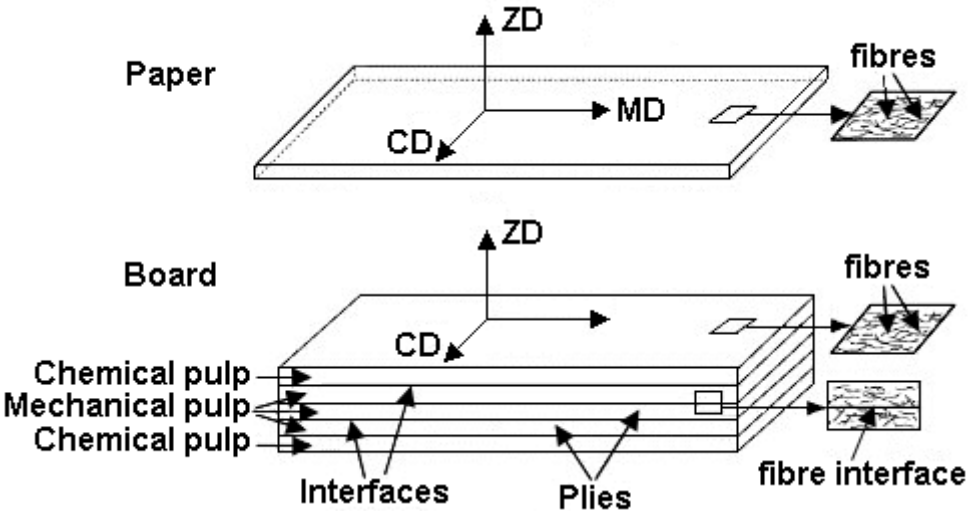

Figure 2.5. Illustration of a single layer paper sheet and a multi-ply board sheet. The cross-direction (CD), machine-direction (MD) and thickness direction (ZD) of the sheet is also defined. Adapted from Xia et al. [36].

When delivered by the headbox onto the forming wire, the pulp suspension consists of around 1% wooden fibres and 99% water and has a temperature of 40-50°C. After the following dewatering in the wire section, the web consists of around 20% wooden fibres and 80% water. Thus, the removal of water is a main process in paper production. The amount of water in the web may be described by the moisture ratio *MR*:

$$\mathrm{MR} = \frac{\mathrm{m}_{\mathrm{water}}}{\mathrm{m}_{\mathrm{fibres}}} \qquad \text{(eq. 2.7)}$$

where m_{water} is the mass of water in the web and m_{fibres} is the mass of fibres. The value of the moisture ratio scales linearly with the amount of moisture in the sheet. Alternatively, the solids content *SC* may be used to quantify the amount of moisture in the web:

$$\mathrm{SC} = \frac{\mathrm{m}_{\mathrm{fibres}}}{\mathrm{m}_{\mathrm{water}} + \mathrm{m}_{\mathrm{fibres}}} = \frac{1}{\mathrm{MR} + 1} \qquad \text{(eq. 2.8)}$$

In the next section of a paper machine, the press section, water is mechanically squeezed out the web through pressing between press felts, see *Figure 2.6*. After the press section the solids content is 40-50%.

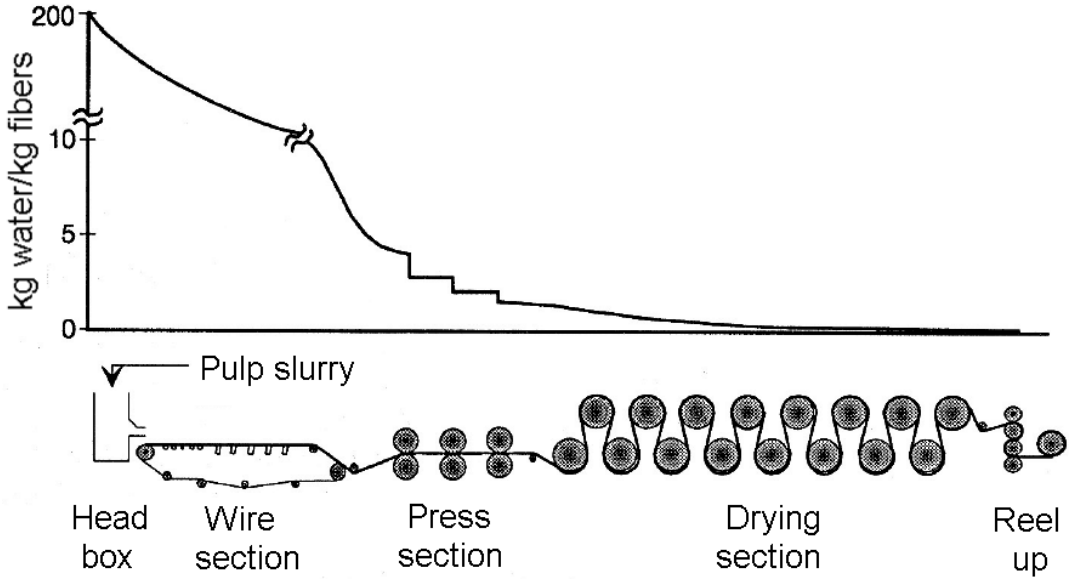

Figure 2.6. Schematic of the water removal process on a Fourdrinier paper machine [37].

In the drying section, most of the remaining water is evaporated from the paper through contact drying on hot cylinders. The energy is supplied to the sheet at its surface. Drying requires heat energy of the order of the heat of evaporation of water. The required heat is partially taken from the web, lowering its temperature in a process known as evaporative cooling. In the drying section, the web temperature will be typically between 50°C to 100°C. However, due to evaporative cooling, the surface temperature may not be the same as that inside the sheet. After drying the paper may be calendered, where the sheet is pressed between heated smooth cylinders to produce a smoother and more compressed sheet, and coated, which implies an additional drying process, before being reeled up onto a pope roll. Here, the solids content will be around 95% [38]. At this stage, the paper is

considered dry, though it has a small amount of moisture when at equilibrium in a conditioned room (23°C, 50% RH). To be considered fully dry (bone-dry) according to industry standards, the paper has to be dried for 24 hrs at 110°C.

The paper production process can introduce undesired variations of properties of the sheet in many ways. For example, variations may be introduced before the headbox, during mixing of the pulp. Here, fibres and additives may bundle together, resulting in uneven distribution of fibres or other components in the sheet. Variations can also be caused in the headbox nozzle before the suspension is delivered onto the forming wire. In addition, uneven structures in the forming wire, press felt and drying fabric may reflect themselves in the final product, resulting in variations in moisture and temperature. These process variations may cause problems during production, and also cause quality variations in the final product.

Non-uniform drying is another example of variations. It can be caused by moisture variations in the web before the drying process. Non-uniform drying may result in quality problems such as out-of-plane deformations [39]. In *Figure 2.7,* an illustrative example of out-of-plane deformations in the ZD direction due to non-uniform drying is shown.

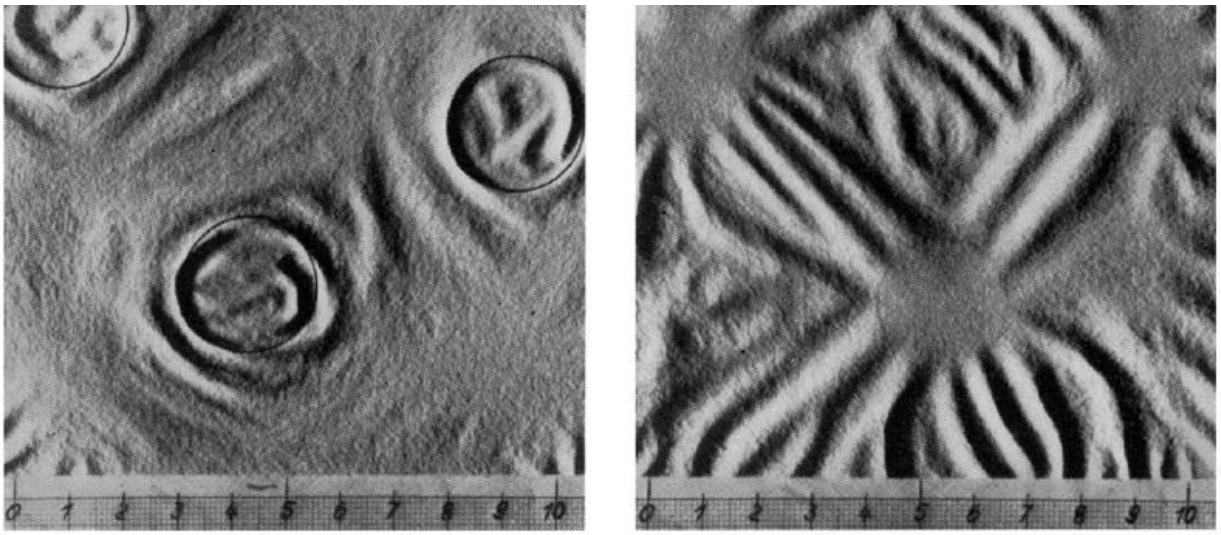

Figure 2.7. Out-of-plane variation (cockling) due to non-uniform drying; adapted from Brecht [40]. Left image: previous to drying, the circles were drier than the surroundings. Right image: previous to drying, the circles were wetter than the surroundings.

A combination of high web tension, lower strength properties of the web due to local variations, and defects in the web can cause web breaks during the production process. A web break results in a production stop. Value losses due to quality problems are large since a large amount of paper may be produced before the problem is detected and corrected. Non-destructive monitoring is used in the production line to predict and detect production problems and to control product properties, for example web grammages, moisture content, temperature, and thickness. The sensors are usually “spot meters” (1D detectors) traversing in the cross-direction of the web. Due to the high production speeds, online traversing spot-meters measure significantly less than 1% of the total web area. The sensors also need some integration time to show a measurement result and are, when put in relation to the production speed, rather slow. Thus, most of the variations may either remain undetected, or the quantitative deviation is significantly underestimated.

Given the technological advances in new detector technology, efforts are being made to develop and introduce online 2D measurement systems with sufficient spatial and temporal resolution as to detect localized variations. Hole detectors, where the web is imaged in the visible wavelength range to detect strongly deviating artefacts, are one example [41]. The use of thermography is another example. An example of local variations detected with 2D thermography at the end of the drying section of a sack paper machine is shown in *Figure 2.8*.

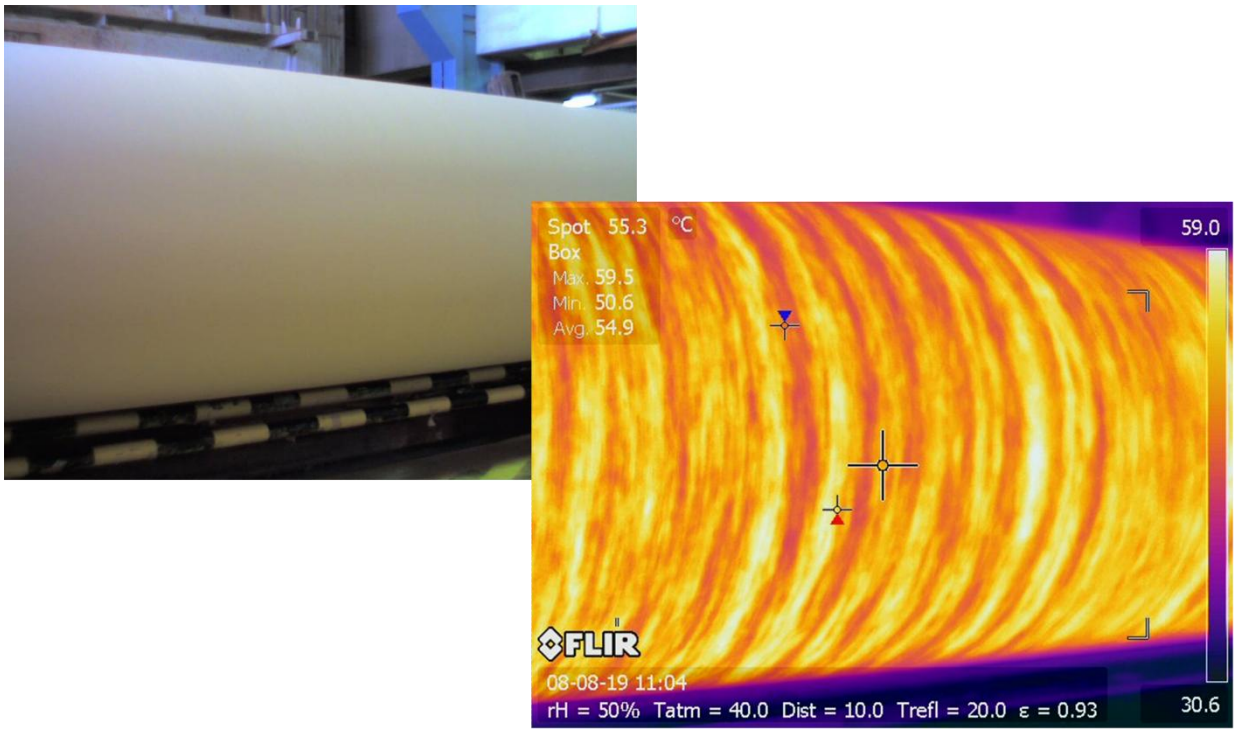

Figure 2.8. Visual (left) and infrared (right) image of the paper web at the end of the drying section of a paper machine, showing temperature variations in the machine-direction and cross-direction.

While online use of thermography in the pulp and paper industry is still under development [42], the technique has been used on many occasions for more than 30 years, for example for analysis of the production process [43-45], or research related to different product properties [46-48]. Thermography has also been used to link the heat generation during the deformation and rupture of paper with the mechanical behaviour of paper [48-51].

The main use of thermography in the pulp and paper industry has so far been qualitative monitoring, rather than quantitative measurements. This can partly be explained by the higher demands needed for quantitative measurements. For accurate results, the temperature of the environment, the humidity of the air, and the emittance of the material need to be known. Another possible explanation is that qualitative measurements, i.e. monitoring trends and variations, are believed to give sufficient information. In qualitative comparisons, emittance and environmental factors are less important. Practical limitations such as the fact that it has been difficult for the thermographic user to single-handedly measure paper emittance can also explain the limited use of quantitative measurements [49].

The emittance of dry paper and board has been reported for parameters such as wavelength [17, 29, 31] and grammage [17]. In many cases, detailed information about the samples (e.g. composition, grammage) has not been given. For dry paper and board, emittance values between 0.61 and 0.92 have been reported, and the values were generally lower in the MWIR range than in the LWIR range, i.e. the emittance of paper increases with wavelength between these regions [17, 29, 31]. The emittance was also found to increase with increasing grammage, especially in the MWIR range [17].

The emittance of moist paper has been investigated for parameters such as moisture content [17, 30], calendering, basis weight, two-sidedness, and whether the pulp was never-dried or dried and repulped [30]. In one of the studies, the trend was that the emittance decreased with increasing moisture ratio [30]. In the other study, the trend was the opposite [17]. Thus, based on the previous studies, the influence of the moisture content on the emittance of paper is inconclusive. In the literature review of this work it was also noted that the emittance of moist paper has not been published for different temperatures or observation angles, nor has it been well investigated in the LWIR range.

When investigating moist paper it is reasonable to compare it with the emittance of water. The emittance of liquid water is high, with values of the normal emittance reported between 0.97 for the MWIR range [52], and 0.98-0.99 for the LWIR range [53-55].

Since the emittance of water is higher than that of paper, it is expected that the emittance of moist paper is higher than that of dry paper. Some studies have commented on the applicability of a "mixing rule", i.e. if the emittance of moist paper can be predicted by a linear, mass share based combination of the emittance of dry paper and the emittance of water [17, 30]. According to the mixing rule, the emittance ε_{mix} of a moist sheet would be:

$$\varepsilon_{\text{mix}} = \frac{\text{MR} \cdot \varepsilon_{\text{water}} + \varepsilon_{\text{fibres}}}{\text{MR} + 1} \qquad \text{(eq. 2.9)}$$

where *MR* is the moisture ratio (see *eq. 2.7*), ε_{fibres} is the emittance of a dry sheet made from the same pulp, and ε_{water} is the emittance of pure water. In the mentioned studies, it was concluded that a simple mixing rule could not be used to predict their measured emittance values. In one of the studies, fibre/water interactions such as fibre swelling were suggested to non-linearly influence the propagation of infrared radiation in the paper [17]. In the other study, a non-linear mixing rule was suggested, with constants that varied with moisture ratio [30].

Many applications of thermography require the sample to be approximately opaque ($\tau \approx 0$). The infrared transmittance of dry [17, 56] and moist [17, 57] paper has been reported in a few studies. In the LWIR range, the reported transmittance was always lower than 0.05. In the MWIR range, the transmittance was less than 0.05 for moisture ratios greater than 1.0 or grammages greater or equal than 60 g/m^2. Thus, in many cases, an assumption of opaqueness is valid when enough samples with grammages or moisture ratios in this range are used.

3 Experimental

3.1 Development of a goniometric setup for emittance measurements

As already stated, quantitative thermographic measurements require knowledge of the emittance of the material. It is of course beneficial to use an emittance adapted to the wavelength sensitivity of the camera sensor, i. e. the integrated and directional emittance. No established method of measuring the integrated and directional emittance of paper existed when this work started. Thus, the first objective was to develop a new method for that, which is described in detail in *Paper A*.

Of the emittance measurement methods mentioned in the previous sections, reference temperature or reference emitter methods are the most easily adapted ones to measure integrated emittance. Hence, the reference emitter methodology was chosen, i.e. the radiation from a sample is compared to that from a reference surface with known emittance under otherwise identical conditions. Ambient radiation emitted from the surroundings is measured by imaging this radiation in a rough, high-reflectance surface at the same position as the samples. The emittance of the sample material can then be determined based on the measured directional radiance of the sample, high-reflectance surface, and reference surface, according to:

$$\varepsilon_{\text{sample}} = \varepsilon_{\text{ref}} \frac{U_{\text{sample}} - U_{\text{amb}}}{U_{\text{ref}} - U_{\text{amb}}} \qquad \text{(eq. 3.1)}$$

where ε_{ref} is the emittance of the reference surface, U_{sample} is the signal voltage from the sensor due to the emitted directional radiance of the sample, U_{amb} is the signal voltage from the sensor due to the emitted radiance of ambient surroundings, reflected into the sensor by the high-reflectance surface, and U_{ref} is the signal voltage from the sensor due to the emitted directional radiance of the well-established emittance reference kept at the same temperature as the sample. Here, it is assumed that the infrared scattering of the ambient radiation by the paper samples, the rough high-reflectance surface, and the reference surface are similar.

The developed emittance measurement method should allow for variation of the observation angle between sensor and samples, in order to study the emittance as a function of observation angle. This angle, θ, is defined as the angle between the optical axis of the sensor and the normal to the measured sample surface, see *Figure 3.1*. Additionally, the temperature of the samples should be well-controlled, in order to establish the influence of temperature on the emittance. Controlling the temperature of the samples allows for improved signal (U_{sample}) to noise (U_{amb}) ratio, for example by elevating the temperature of the samples well above the temperature of the surrounding room. These issues were all carefully addressed by the design and construction of an angle-resolved goniometer shown in *Figure 3.1*. As can be seen it is adapted for pivoting an infrared camera around the sample holder that is located in a temperature-controlled

oven. The camera can be positioned at an arbitrary observation angle in the range $90° < \theta < 90°$.

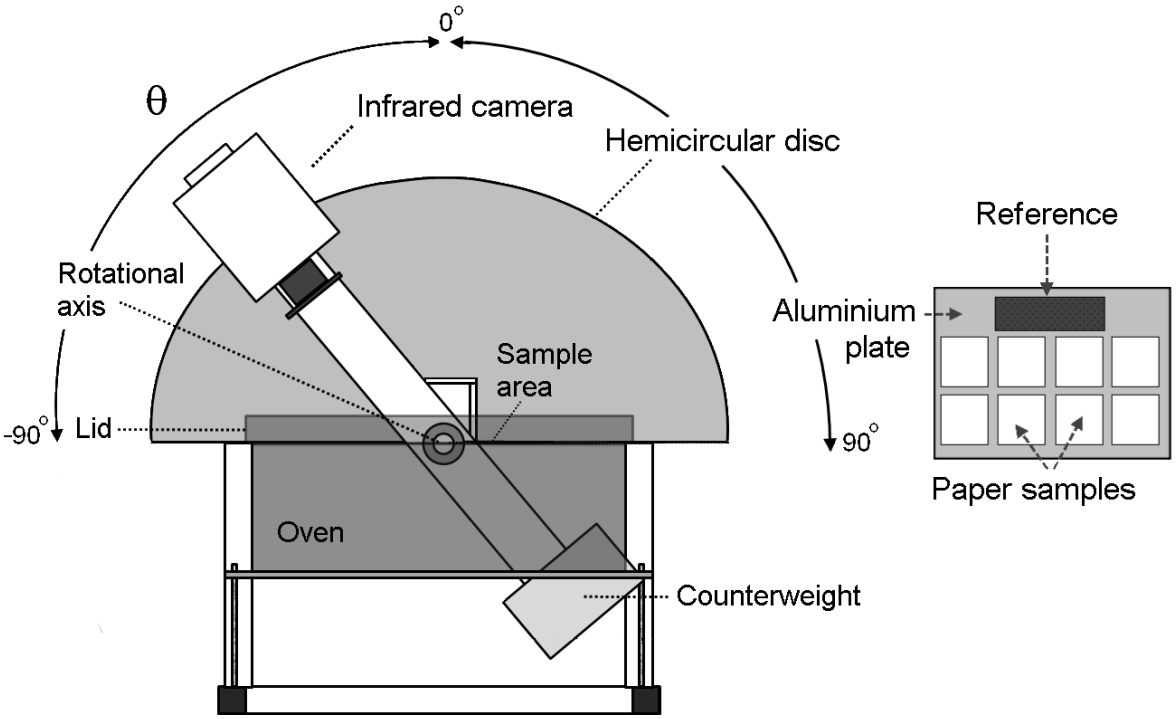

Figure 3.1. Illustration of angle-resolved goniometer for emittance measurements. Also shown is the oven for heating of the paper samples, the emittance reference surface, and the high-reflectance surface.

The samples to be measured are taped onto an aluminium plate using temperature resistant tape. The emittance reference surface is positioned next to the samples, see *Figure 3.1*. The samples and reference are then placed in the oven and heated to the desired temperature (usually 70°C). The high-reflectance surface is kept outside the oven during heating of the samples. When the influence of temperature on the emittance is investigated, the temperature can be controlled to an uncertainty of ±0.3°C in the temperature range between 30°C and 100°C. An inclinometer is used to position the camera at the desired observation angle. Unless the directional dependence (dependence on observation angle) of the emittance is studied, normal observation angle ($\theta = 0°$) is the default. As different infrared cameras can be attached to the goniometer arm, the influence of wavelength range (MWIR and LWIR) on the emittance can be studied.

When the samples have reached equilibrium in the oven at the desired temperature, the lid of the oven is removed, and the samples and reference are imaged by the infrared camera, see *Figure 3.2*. Typically, fully uncovering the lid takes 0.3 s, and nine infrared images are captured during this time. Next, the high-reflectance surface is placed at the same position as the samples, and the image of the surrounding radiation is captured before it is removed. The samples are then heated again, and the temperature or observation angle is adjusted according to the next measurement. The stored infrared images are then analysed with the software provided by the camera manufacturer, in order to extract the signal voltage from the infrared images of the paper samples, reference and high-reflectance surface. Here, the signal voltage from the samples and reference may be extracted from consecutive frames during the retraction of the lid (*Figure 3.2*), or from the same image frame when both samples and reference are fully

uncovered. *Eq. 3.1* is then used to calculate the emittance of the samples. Five measurements are performed on the same samples, and the measured emittance values from the five measurements are averaged to produce the final result.

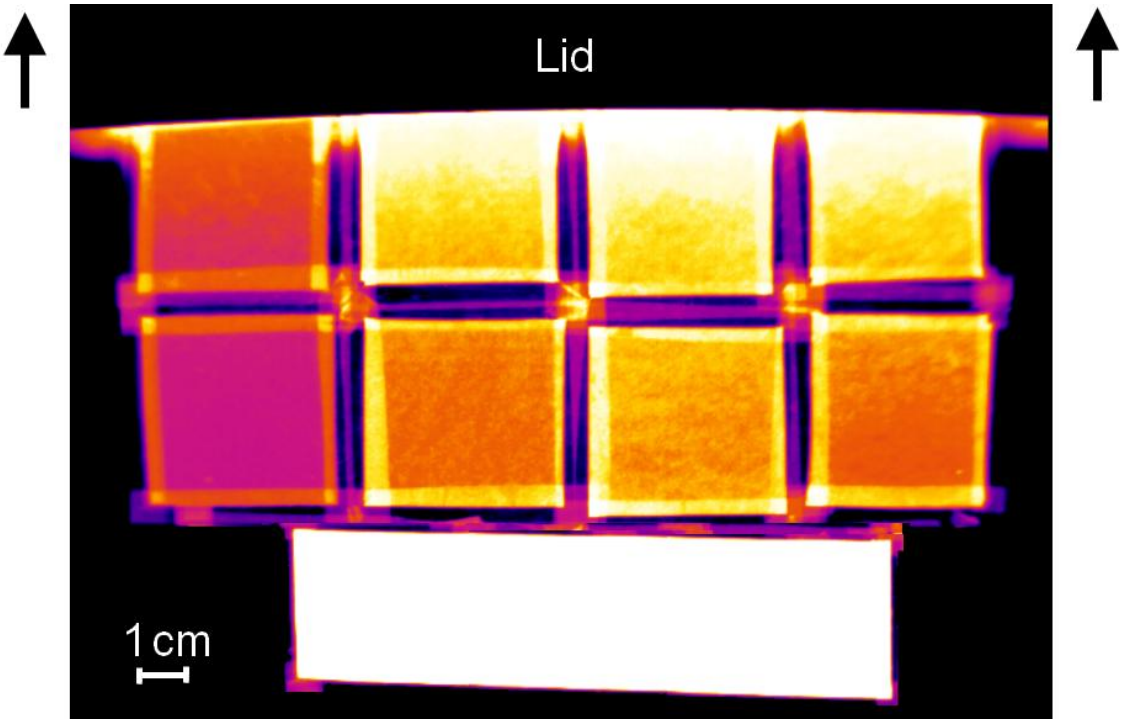

Figure 3.2. Infrared image of the opened oven and samples, with the reference surface (white area at bottom), the two sample rows, and the retracting lid of the oven (black area at the top), as viewed with the SC6000 MWIR camera. The physical scale of the image is also indicated.

The applicability of the developed emittance measurement method was evaluated by measurements on dry paper samples (grammage 60 g/m^2) made from thermo-mechanical pulp (TMP). A high-emittance coating (Nextel Velvet from Mankiewicz; ε_{MWIR} = 0.93 ± 0.01, ε_{LWIR} = 0.96 ± 0.01) was chosen as emittance reference. The Nextel coating was painted in five layers on an aluminium plate. A rough gold surface (Infragold from Labsphere, ρ = 0.94-0.96) was used as the high-reflectance surface for ambient radiation measurement. Two infrared cameras were used, both at a frame rate of 30 Hz; a FLIR SC6000 MWIR camera, sensitive between 3.0 and 5.0 µm, and a FLIR SC640 LWIR camera, sensitive between 7.5 and 13.0 µm. Both cameras were specified to have a measurement uncertainty of ±2.0°C, or 2% of the signal voltage. While it was mentioned by the manufacturer that the uncertainty in practice was much lower (less than 0.06°C) if the cameras were used under controlled conditions and for repeated measurements on similar objects, the higher specified uncertainty was used in the error analysis of this thesis work. To position the camera at the desired observation angle, a Digital Angle Gauge inclinometer from Wixley (measurement uncertainty ±0.1°) was used.

In the evaluation of the method, sample temperature, wavelength range, and observation angle was varied. The observation angle θ was varied in a sequence from 0° to -80°, and then from 0° to 80°, in increments of 10°. The two sequences were then averaged to produce a single angle-resolved sequence from 0° to 80°. Measurements were performed on stacks of 1, 3 or 5 samples, in order to estimate the possible effect of transmittance on the results. In order to verify the emittance results obtained with the developed method,

an alternative emittance measurement method, FTIR spectrophotometry, was used on the same samples. The obtained results were also compared to paper and board emittance values measured by other authors [17, 30, 31].

An error analysis of the emittance measurement method was made, which is presented in detail in *Paper A*. The accuracy of the method was theoretically estimated by mean error propagation of *eq. 3.1*. The estimation included the uncertainty of the camera sensor, emittance value of the reference surface, and software analysis procedure used to extract the signal voltage values from the samples, respectively, mentioned in order of their estimated impact. Here, the estimated uncertainty in emittance for samples measured at normal angle and at temperature 70°C was ±0.02 in the MWIR range, and ±0.03 in the LWIR range. The repeatability of the method was evaluated by calculation of the standard deviation from five identical measurements made on the same sample. The obtained standard deviation σ at normal observation angle was ±0.01, while it increased to 0.02 at grazing angles, where the uncertainty in the angular positioning of the camera had a greater impact on the measurement result. The total uncertainty of the measured emittance values was taken to be the sum of the mean error propagation and the calculated standard deviation. Thus, the total uncertainty at 1σ level in measurements of normal emittance at 70°C was estimated to between ±0.03 ($\theta = 0°$) and ±0.04 ($\theta = 80°$) in the MWIR range, and between ±0.04 ($\theta = 0°$) and ±0.05 ($\theta = 80°$) in the LWIR range.

3.2 Emittance measurements of paper

Previous studies on the emittance of dry and moist paper and board were found to be incomplete, and the reported results sometimes contradictive. The angle-resolved goniometric emittance measurement method that was developed during this thesis work (*Paper A*) was utilized to measure the directional integrated emittance of several dry and moist paper and board samples (*Paper B*). Product properties such as pulp type, refining, drying of the pulp, fibre orientation and coating were varied.

Dry paper and board samples were obtained as handsheets or industrial sheets. Handsheets (60 g/m^2) of the pulp types listed in *Table 3.1* were prepared: TMP, bleached softwood, unbleached softwood, birch, and a mix of birch and softwood. Sheets were made from both dried and never-dried birch pulp, which was either unrefined or refined (80 kWh/t). The handsheets were assumed to be isotropic in the MD-CD plane (see definitions in *Figure 2.5*). Industrial sheets comprised sack paper, coated three-ply board, and uncoated two-ply linerboard. Here, samples were arranged so that the influence of fibre orientation (MD and CD) on the directional emittance could be observed. In general, samples were chosen as to be representative of either different parameters in the papermaking process, such as fibre treatment or coating, or of the use of the finished product.

Sample type	*Abbreviation*	*Preparation*
Thermo-mechanical (newsprint)	TMP	Handsheets
Softwood + birch	Mix	Handsheets
Birch	Birch	Handsheets
Bleached softwood	BSW	Handsheets
Unbleached softwood	USW	Handsheets
Uncoated linerboard – bottom side	UcB	Machine made
Uncoated linerboard – top side	UcT	Machine made
Coated board – bottom side	CB	Machine made
Coated board – top side	CT	Machine made
Sack paper	SP	Machine made

Table 3.1. Summary of dry sample types used in emittance measurements.

Moist handsheets with a difference in moisture ratio were prepared using an adapted pressing procedure. Bleached and unbleached softwood pulp was used, and the moisture ratio of the sheets was determined gravimetrically. The moist sheets were then wrapped in a thin plastic film in order to prevent evaporative cooling during the measurements.

The emittance of the dry and moist samples was measured using the new goniometric setup described earlier in this chapter. All sample types were investigated in both the MWIR and the LWIR range, at a temperature of 70°C, and the observation angle was varied for all sample types except the sack paper, which was only measured at normal angle. After the measurements, the moist samples were weighted in moist and bone-dry condition. Here, it was found that some moisture leakage occurred during the course of sample heating and measurement (5-7 hrs). Calculations suggested that the moisture had leaked through the seal of the plastic wrap at an approximate rate of 0.60 mg/min,

causing the measured emittance to deviate by up to 0.12 from its estimated true value. In the subsequent analysis, a compensation for the moisture leakage was made. The compensation was based on the observed decrease in the emittance as a function of time during a measurement sequence, and on the interpolation of data from points during the sequence where the moisture ratio was measured, and hence well-known.

A separate compensation was made to account for the infrared absorptance of the plastic film and its influence on the directional dependence. These effects were estimated to introduce an error between 0.02 and 0.15 to the measured emittance, dependent on wavelength range an observation angle. The compensation was based on a comparison of the measured signal voltage of from a wrapped and a non-wrapped sample.

The compensations introduced additional uncertainty to the measurements. The introduced uncertainty in the emittance due to the moisture leakage compensation was estimated to be between ±0.01 ($\theta = 0°$) and ±0.04 ($\theta = 80°$). The corresponding uncertainty in the compensation of the infrared absorptance of the plastic film and its influence on the directional dependence was estimated to be between ±0.01 ($\theta = 0°$) and ±0.03 ($\theta = 80°$). The uncertainties due to the compensations were then added to the total estimated uncertainty for the measurements on dry samples, as described in the previous section. Additional details of the compensations and an error analysis of the measurements on moist samples are given in the appendix of *Paper B*.

3.3 Determination of energies during paper deformation

The developed goniometric setup for emittance measurements has been demonstrated to be a valuable tool for the determination of more accurate paper emittance values under different conditions. However, the system with its improved accuracy has a great potential also in analysing other phenomena. This was demonstrated in *Paper C*, where precise emittance values and quantitative thermography provides new insights into the deformation behaviour of sack paper samples.

A Material Testing System (MTS) was used to perform a uniaxial tensile test on industrially manufactured sack paper samples (width 50 mm, length 100 mm, grammage 68 g/m^2) in the MD and CD directions, respectively. The samples were attached to clamps and pulled at a constant deformation rate of 0.3 mm/s. The deformation of the sample progressed from the initial elastic, or reversible, regime, through the plastic, or irreversible, regime, and up to the point of rupture, see *Figure 3.3*.

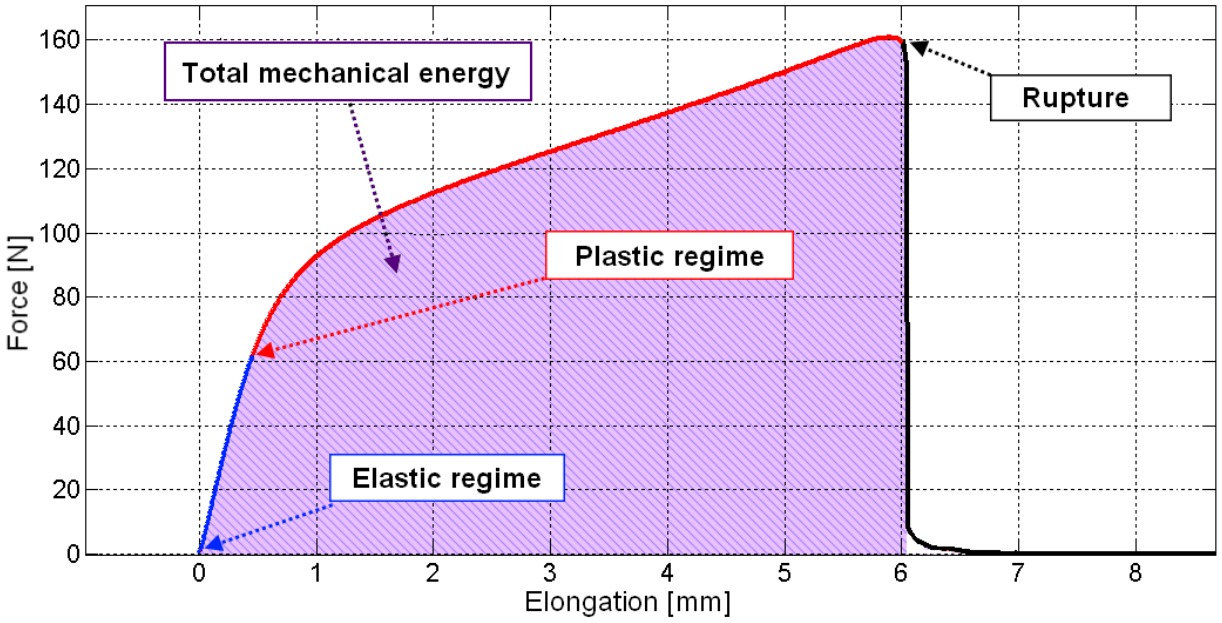

Figure 3.3. Force-elongation curve of a sack paper sample during a tensile test, with indications of the elastic (blue part of the curve) and plastic (red part of the curve) regimes of the deformation, the point of rupture, and the total mechanical energy at the point of rupture (purple shaded area).

During the tensile test, an infrared image sequence was simultaneously obtained by the SC6000 MWIR camera, used at a frame rate of 32 Hz for the MD samples and 55 Hz for the CD samples. Several steps were taken to ensure accurate thermographic data. The measurements were performed in a climate-controlled room (T_{air} = 23°C, 50% RH). The ambient radiation from the surroundings was obtained using the high-reflectance surface, and the emittance of the sack paper was determined using the new goniometric setup.

Using the measured force/deformation and temperature data, both the total mechanical and thermal energy as a function of time could be determined. The thermal energy was calculated given the measured emittance of the sack paper, a specific heat value based on literature values, and the average emitted spectral radiance from the entire sample as

measured by the infrared camera. *Figure 3.4* presents a visual image of the sample prior to testing and a thermographic temperature image of it at the time of rupture.

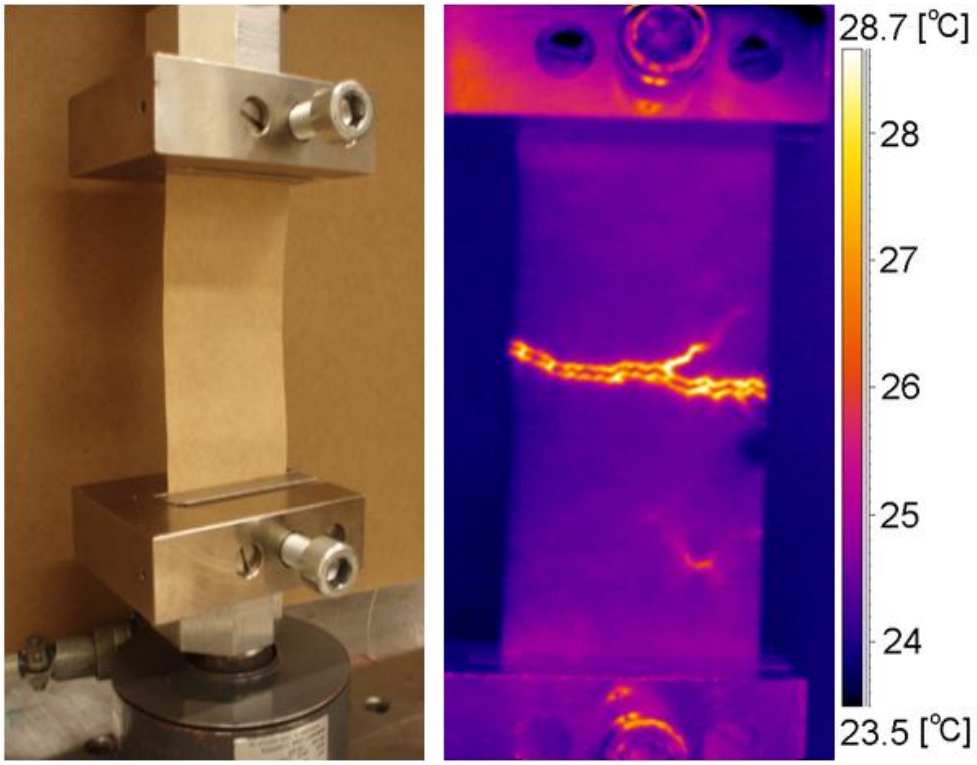

Figure 3.4. Visual image of paper sample attached to clamps in a Material Testing System (left), and infrared image of sample at time of failure (right).

The total mechanical energy was calculated as the area under the force-elongation curve, see *Figure 3.3*. From the total mechanical energy, the plastic and elastic part of the energy as a function of time was calculated. The calculation is presented in detail in *Paper C*.

Given that the camera recording and the MTS displacement were not synchronised to the timing of single frames, the data sets were aligned as a function of time under the assumption that the maximum temperature of the sample coincided with the time of failure, i.e. when the maximum forces were applied to the sample.

4 Results and discussion

4.1 Applicability of the goniometric method

The results and conclusions of the evaluation of the developed goniometric setup were reported in *Paper A*, and are also summarized below. Taking into account the methodological differences between the two measurement approaches (angle-resolved goniometric and FTIR), the results were in good agreement. No impact of the sample transmittance on the results was observed, and FTIR measurements confirmed that the transmittance of the samples was low. However, the observation was made that for samples of lower grammage than 60 g/m^2, measuring on a stack of at least 3 samples would be advisable. For illustrative purposes, a sample of greaseproof paper (37 g/m^2), was measured with FTIR, and its reflectance, transmittance and emittance was compared to that of TMP, see *Figure 4.1*.

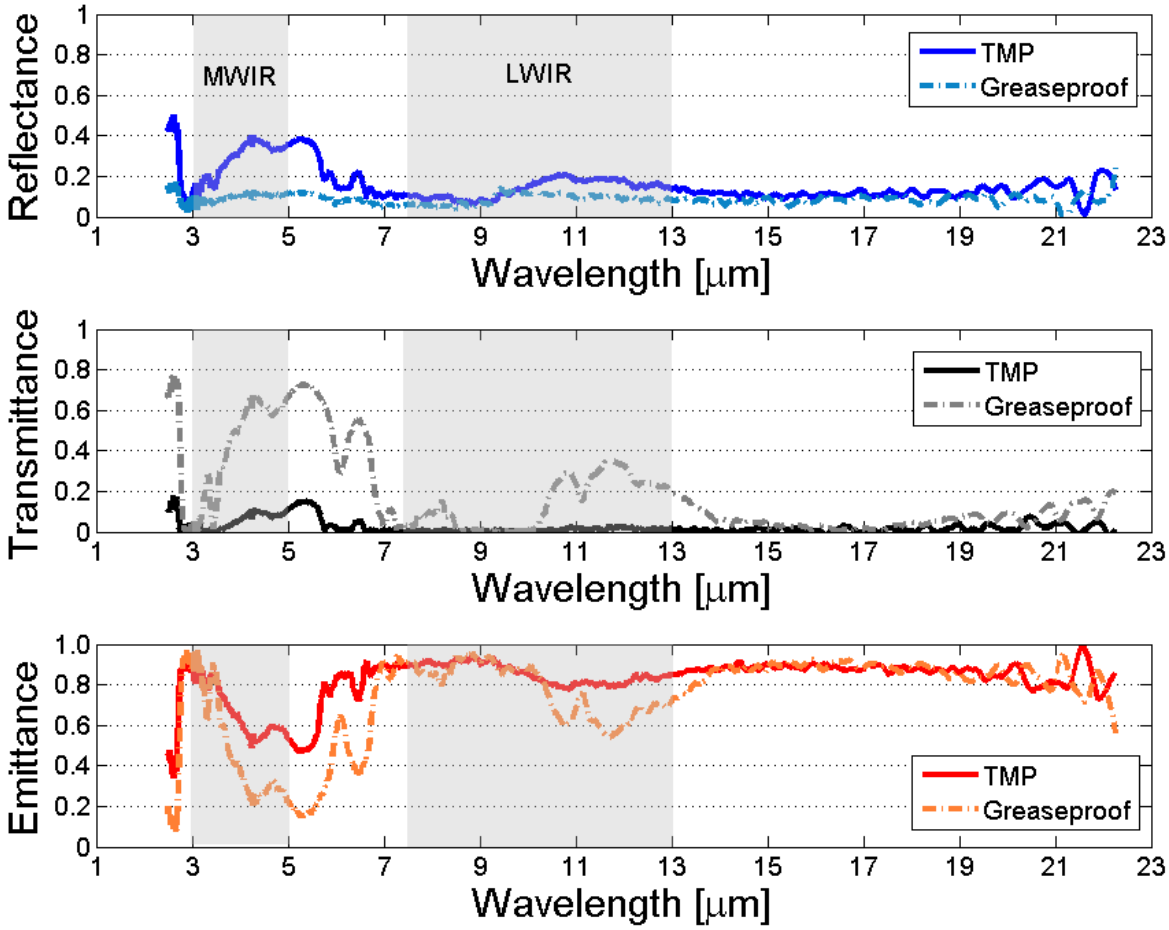

Figure 4.1. Spectral and hemispherical reflectance, transmittance and emittance of greaseproof (37 g/m^2) and TMP (60 m/m^2) samples, derived from FTIR measurements, with the MWIR and LWIR ranges indicated. The measurement uncertainty is ±0.02 for the reflectance and transmittance values, and ±0.03 for the emittance values.

After completion of the evaluation of the goniometric setup, some improvements of the method were done. For example, it was found that the results were sensitive to the total time of heating before measurements were started. A heating time of at least 2½ hours was needed for samples, reference and oven to reach equilibrium at the desired temperature. Otherwise, the first few measurement points would exhibit a slightly lower emittance than subsequent measurements. It was also found that the samples and reference cooled rapidly (about 0.002°C/ms) when, at the time of measurement, the lid of the oven was removed and the samples and reference were exposed to air. To compensate for that, each row of samples and reference should be analysed as they are subsequently uncovered by the lid and exposed to the cooling air and the camera sensor (see *Figure 3.2*), and not simultaneously in the same image frame. Additionally, the reference surface should be prepared as a Nextel-painted paper surface, and not a Nextel-painted aluminium surface, in order to achieve similar cooling and surface scattering properties for the samples and reference. These corrections were all done prior to the measurements reported below.

4.2 Measured emittance values

Results from normal (θ = 0°) emittance measurements of dry paper samples in the MWIR and LWIR ranges are shown in *Figure 4.2.* The uncertainty bars derived from the error analysis are discussed in detail in *Paper A.* The standard deviation obtained from identical repeated measurements was typically 0.01.

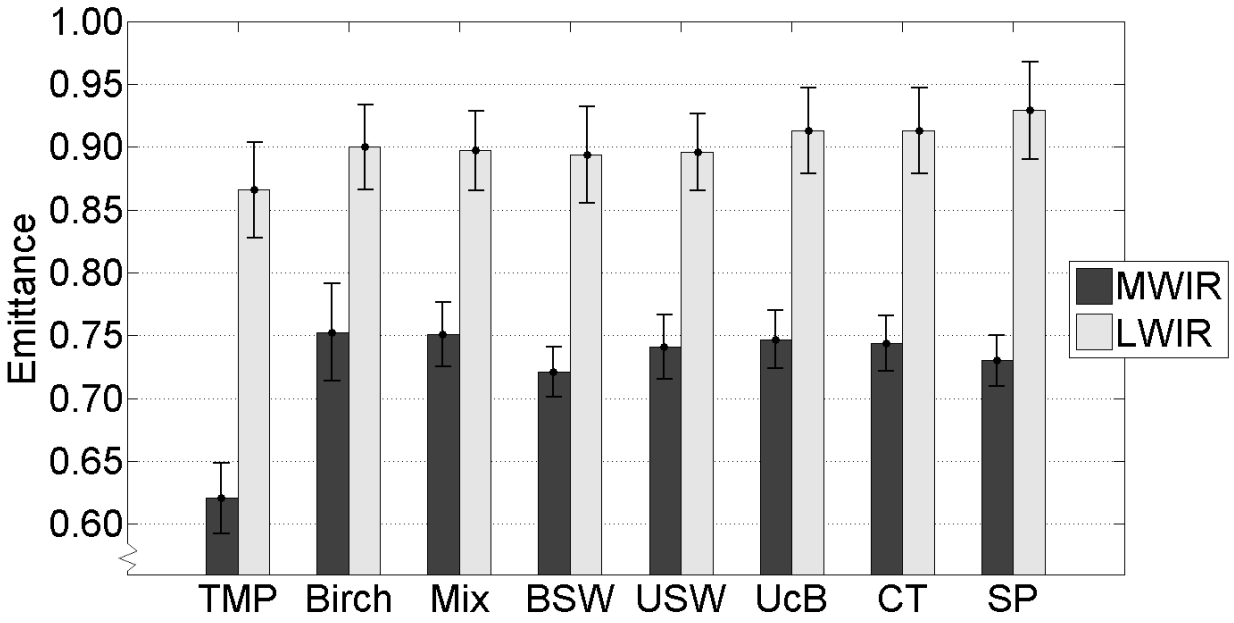

Figure 4.2. Measured normal MWIR and LWIR emittance at 70°C for different samples: TMP, birch, birch and softwood (Mix), bleached softwood (BSW), unbleached softwood (USW), bottom-side uncoated linerboard (UcB), top-side coated board (CT), and sack paper (SP).

The emittance of paper and board was higher in the LWIR range than in the MWIR range, corroborating previous measurement results [17, 29, 31] and the spectral FTIR measurements shown in *Figure 4.1*. In the MWIR range, the emittance of the different pulp types varied by 0.13, from 0.62 to 0.75, with an average value of 0.72. In the LWIR range, the corresponding variation was 0.06, with a lowest value of 0.87 (TMP), and an average value of 0.90. Beating was found to slightly increase the MWIR emittance of the birch pulp samples. Coating was found to increase the MWIR emittance of the board; however, this was likely an effect of the composition of the coating layer. Here, results from the measurements of the never-dried or dried and repulped birch pulp samples are not shown, as no influence was observed.

The MWIR range appears to be more sensitive to variations in pulp properties, compared to the LWIR range. A possible explanation is that absorption lines appear to be more distinct in the MWIR range, see *Figure 4.1*. For example, a strong absorption feature is present around 3.0 μm, which has been attributed to hydoxyl (OH^-) vibrations in cellulose [58, 59], or to small concentrations of absorbed atmospheric moisture [57], which has a strong absorption line at 2.9 μm. When the slope of an absorption line is steep and coincides with the boundary of a wavelength range, small shifts in the line due to variations in chemical composition may impact significantly on the measured integrated emittance.

The influence of temperature on the normal emittance of dry TMP samples was studied in *Paper A*. The results are summarised and presented in *Figure 4.3.*

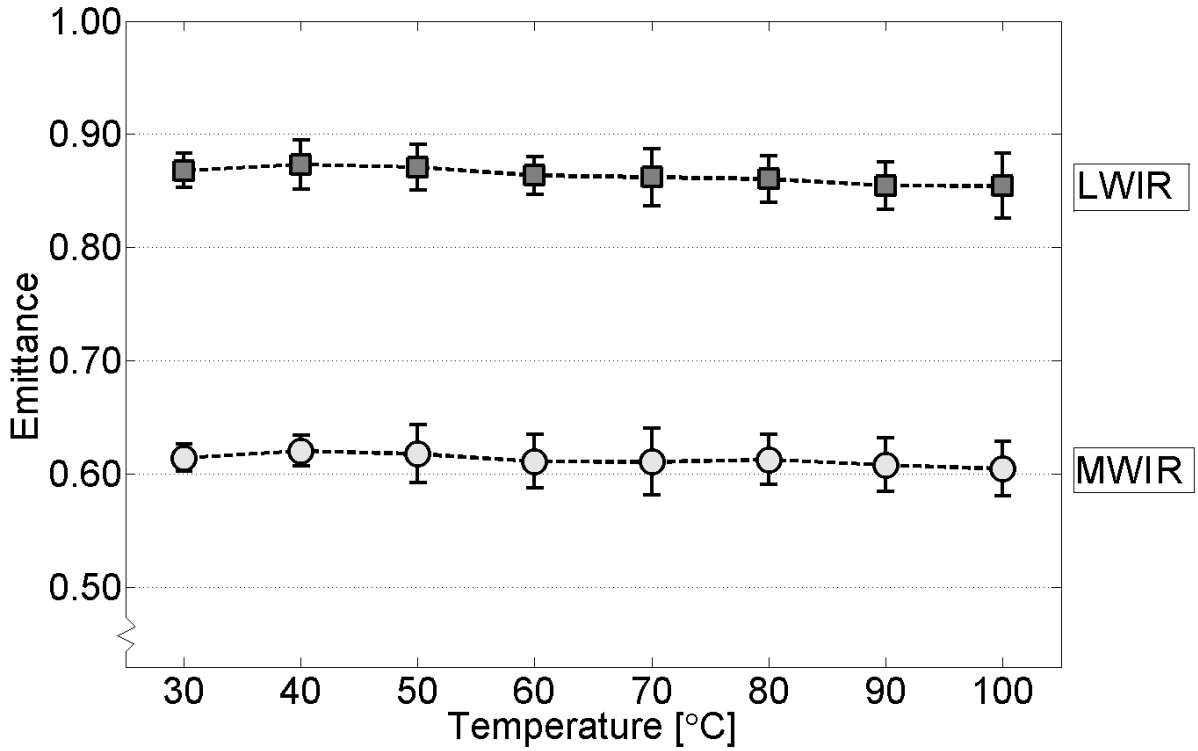

Figure 4.3. Measured normal emittance of TMP as a function of sample temperature, in the MWIR and LWIR ranges. From Paper A.

A can be seen in *Figure 4.3,* there was no significant effect of temperature on the emittance of the TMP samples. Thus, in the following measurements it was assumed that the emittance of paper was independent of temperature, and the reported values were all obtained at a sample temperature of 70°C.

The directional dependence (dependence on observation angle) of the emittance of dry paper, board, and linerboard samples made from different pulps were reported in *Paper B*. *Figure 4.4* and *Figure 4.5* show an excerpt of the results as graphs.

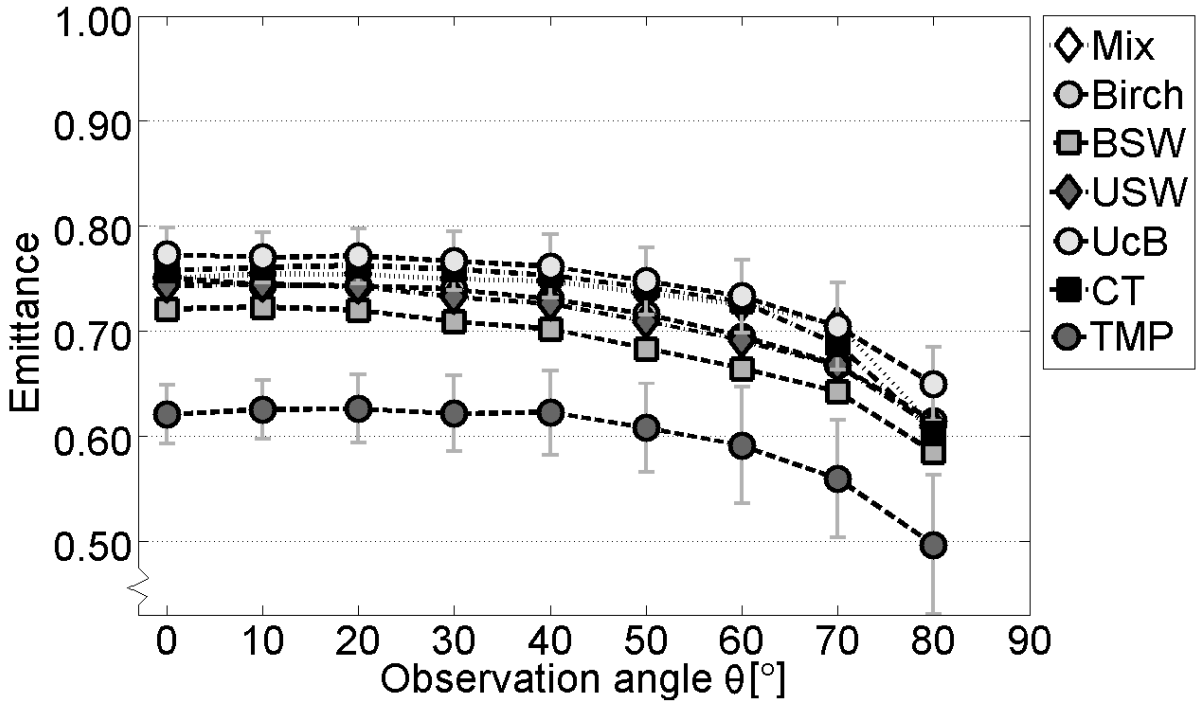

Figure 4.4. Measured MWIR emittance as a function of observation angle for different samples at 70°C: birch and softwood (Mix), birch, bleached softwood (BSW), unbleached softwood (USW), bottom-side uncoated linerboard (UcB), top-side coated board (CT), and TMP; for reference, the uncertainty bars for the sample with the highest and lowest emittance are shown in order to not make up a messy graph.

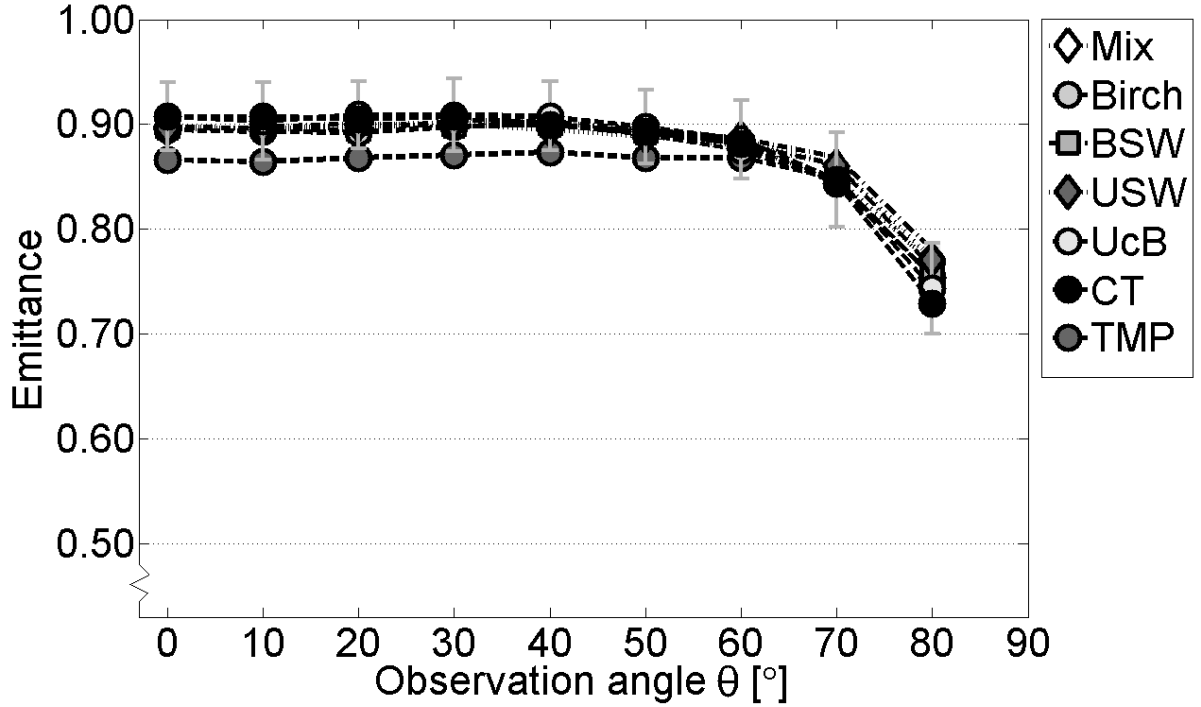

Figure 4.5. Measured LWIR emittance as a function of observation angle for different samples at 70°C: birch and softwood (Mix), birch, bleached softwood (BSW), unbleached softwood (USW), bottom-side uncoated linerboard (UcB), top-side coated board (CT), and TMP; for reference, the uncertainty bars for the sample with the highest and lowest emittance are shown in order to not make up a messy graph.

The directional dependence of the emittance varied with wavelength. In the MWIR range, taking the uncertainty bars into consideration, the emittance was approximately constant up to an observation angle of 60°, after which it started to decrease. In the LWIR range, the decrease started at 70°. On average, for all sample types, the emittance decreased by 0.13 in the MWIR and 0.15 in the LWIR as the observation angle went from 0° to 80°. The directional dependence of the different samples exhibited some differences. TMP had the weakest directional dependence, (decrease of 0.12 in the MWIR and 0.11 in the LWIR) and the top side of the coated board had the strongest directional dependence (decrease of 0.15 in the MWIR and 0.18 in the LWIR). Here, the surface roughness is a possible explanation. A low surface roughness (high smoothness) is expected to increase the directional dependence, and the visual impression was that the top-side coated board had the lowest surface roughness, while the TMP sample had the highest surface roughness.

For the industrially made, oriented board and linerboard samples, it was expected that a possible influence of the orientation of the sheet (MD or CD) would be strongest at grazing angles. However, when comparing results for the measurements in the MD and CD direction of the industrially made samples, no significant difference in emittance was found at different observation angles.

To be able to present emittance values relevant for the papermaking process, where the moisture ratio of the web varies significantly, a thorough investigation of the influence of moisture was made and presented in *Paper B*. These results are summarised *Figure 4.6* to *Figure 4.9*.

The normal emittance of unbleached softwood as a function of moisture ratio is shown in *Figure 4.6* for the MWIR range, and in *Figure 4.7* for the LWIR range. Here, the data was chosen only from the final measurement in each series of consecutive, angle-resolved measurements. As the moisture ratio of the sample was determined directly after this final measurement, both the moisture ratio and the emittance were known, and no moisture leakage compensation was needed. Since the measurements at normal angle were not influenced by the directional dependence of the plastic film, the data was only compensated for the infrared absorptance of the film. In the figures, the estimated emittance ε_{mix} obtained by applying a "mixing rule" *(eq. 2.9)* is also shown, depicted as the thin dashed line.

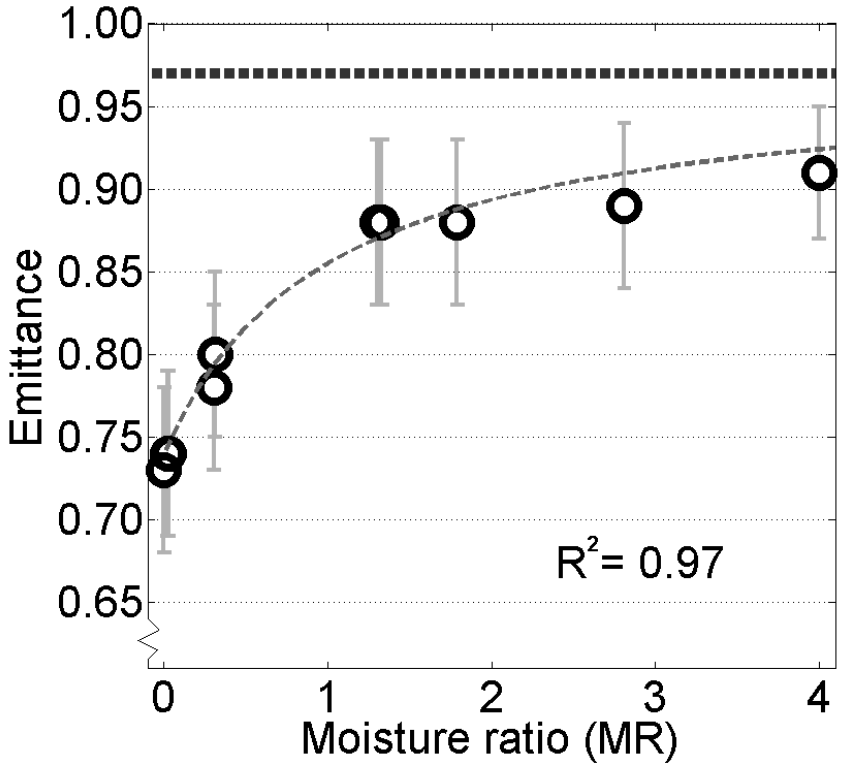

Figure 4.6. Normal MWIR emittance of unbleached softwood paper (USW) as a function of moisture ratio, measured at 70°C. The measured values were compensated for the absorptance of the plastic wrap. The estimated emittance ε_{mix} (thin dashed line), and the emittance of pure water (thick dotted line) are also shown. From Paper B.

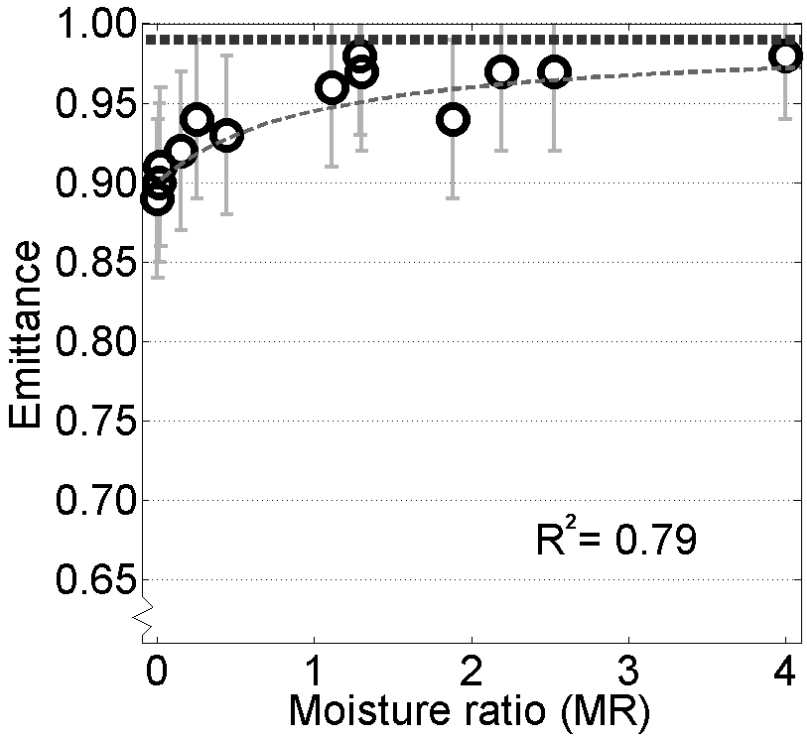

Figure 4.7. Normal LWIR emittance of unbleached softwood paper USW) as a function of moisture ratio, measured at 70°C. The measured values were compensated for the absorptance of the plastic wrap. The estimated emittance ε_{mix} (thin dashed line), and the emittance of pure water (thick dotted line) are also shown. From Paper B.

The emittance of the samples increased as the moisture ratio increased. In the MWIR range, the normal emittance of the wettest samples was 0.18 higher than that of the dry samples. In the LWIR range, the same difference was 0.08, i.e. the LWIR emittance was less sensitive to changes in moisture. That the emittance of a moist sample was higher than that of a dry sample seems logical, given that the emittance of water is higher than that of paper. Correspondingly, one might expect the emittance of a moist sample to obtain values between the emittance of a dry sample and the emittance of pure water.

The normal emittance as a function of moisture ratio complied well with the estimated emittance ε_{mix} for the investigated pulps. The average R^2 value for all measurements was 94% in the MWIR range, and 77% in the LWIR range. Thus, the emittance of a moist sample can be estimated from the emittance of pure water and the emittance of a dry sample, according to *eq. 2.9*. Here, previous studies disagree [17, 30]. However, in the study of Trepanier [30], the influence of evaporative cooling and ambient radiation on the measurement results was not well accounted for. In that study, the emittance decreased as the moisture ratio increased, contrary to the trends seen in this thesis. In the study of Ojala [17], the results agreed with this thesis in that the emittance increased as the moisture ratio increased, a behaviour that has also been reported for materials such as soils [60]. A possible explanation for the conclusion of Ojala that the "spectrum of wet paper cannot be derived merely by counting two spectra together", is that a mass-share based combination was not considered.

Two examples of the emittance of moist paper as a function of observation angle are presented in *Figure 4.8* and *Figure 4.9*. The results for each given moisture ratio were measured as a series of consecutive measurement, where observation angle θ was varied between 0° and ±80°, and during which some moisture leakage occurred. The moisture leakage compensation introduced in the previous chapter was performed on the data to remove the impact of the leakage, see the appendix of *Paper B* for details. Additionally, the data was compensated for the infrared absorptance of the plastic film and its influence on the directional dependence.

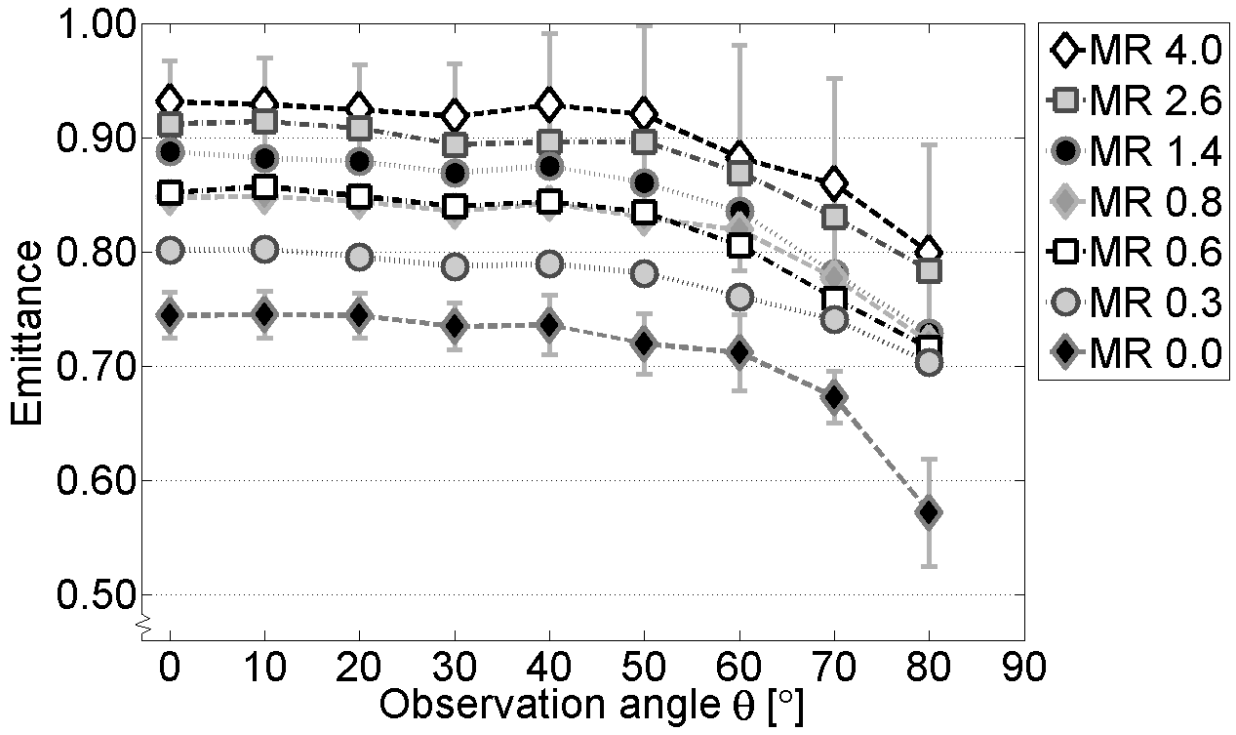

Figure 4.8. MWIR emittance as a function of observation angle for unbleached softwood pulp (USW) with moisture ratio (MR) from 0 to 4.0, measured at 70°C. The measured values were compensated for the absorptance and directional dependence of the plastic wrap, and for moisture leakage. From Paper B.

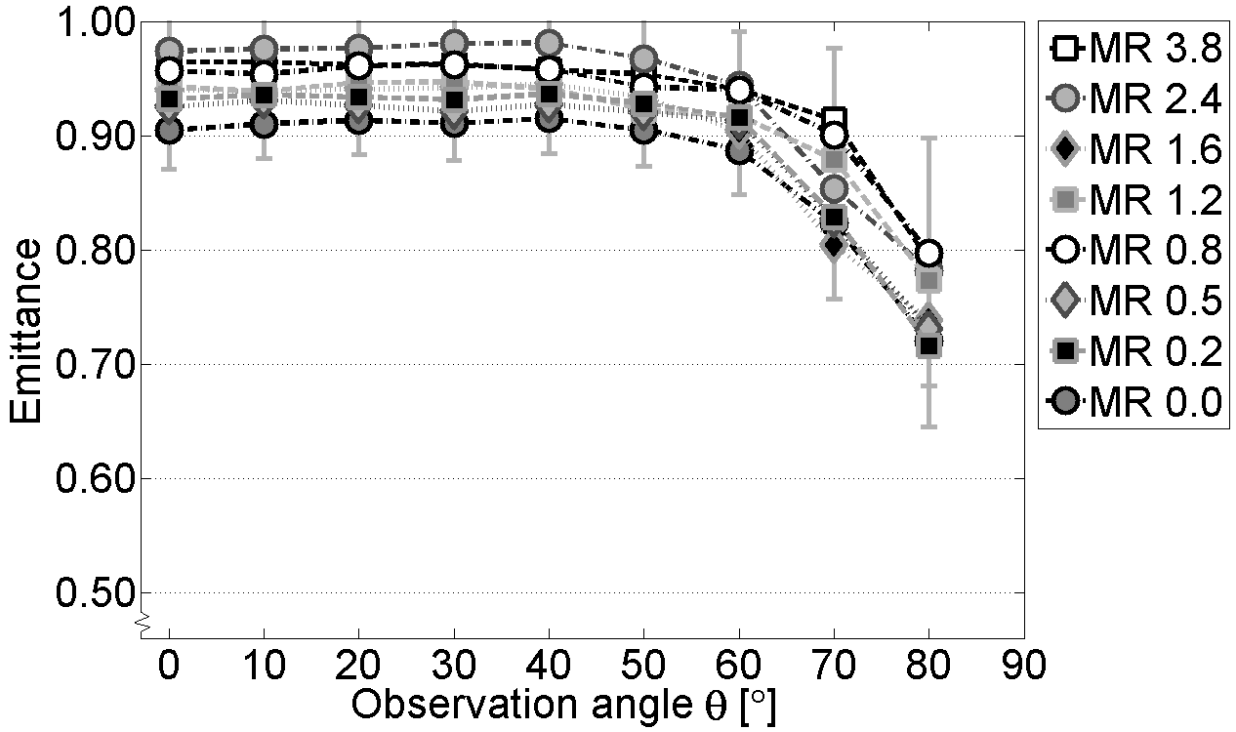

Figure 4.9. LWIR emittance as a function of observation angle for unbleached softwood pulp (USW) with moisture ratio (MR) from 0 to 3.8, measured at 70°C. The measured values were compensated for the absorptance and directional dependence of the plastic wrap, and for moisture leakage. From Paper B.

The MWIR emittance of the moist samples exhibited a slightly stronger dependence on observation angle than the LWIR emittance. It was expected that the wettest samples would exhibit a stronger directional dependence than drier samples, as water is increasingly reflective at grazing angles. Such an effect was not observed. However, the error of measurements of moist sample is large enough at $\theta > 60°$ to obscure minor differences in directional dependence. Additionally, water is only expected to significantly change the directional dependence if it is distributed as mirror-like surfaces, for example in the spaces between the fibres, and close enough to the surface so that emitted and reflected radiation from the water is not obscured by nearby fibres.

4.3 Release of energy during paper rupture

In the previous chapter it was described how an infrared camera was used to obtain an infrared image sequence of the deformation of a sack paper sample during a tensile test. The measured MWIR emittance of sack paper was used to convert the infrared radiance image to a temperature image (*Figure 3.4*, right). From this data, the thermal energy dissipated from the sample during the tensile test could be calculated. The results and conclusions of the study were reported in *Paper C*, and are also summarized below.

During the deformation phase of the tensile test, the temperature of the entire sample increased gradually, before it ruptured with a sharp increase in temperature. Most of the temperature increase occurred in the rupture zone where a temperature increase of up to 6°C was measured, implying that a lot of energy was instantaneously dissipated.

The thermal energy was compared to the plastic and elastic part of the total mechanical energy that was calculated to be stored in the sample at the same time, as described in *Paper C*. *Figure 4.10* presents results of the comparison, for a MD-oriented sample.

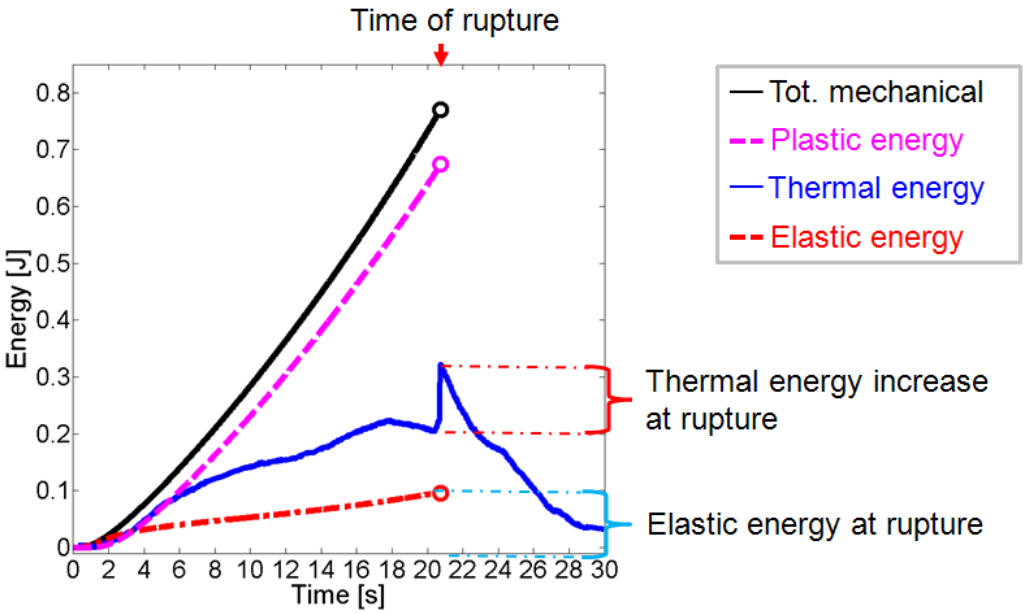

Figure 4.10. Example of the calculated total mechanical, plastic, elastic and thermal energy as a function of time during tensile testing of a sack paper sample oriented in the MD direction.

When comparing the thermal and total mechanical energies at the time of failure, 40 to 60% of the exerted mechanical energy could be detected as an increase in thermal energy. The remaining energy was most likely transferred already during the experiment to the environment due to cooling of the sample.

The sharp increase in thermal energy at the time of rupture was found to correspond well with the elastic energy that was calculated to be stored in the sample. In *Figure 4.11*, the increase in thermal energy and the stored elastic energy are compared for the different experiments.

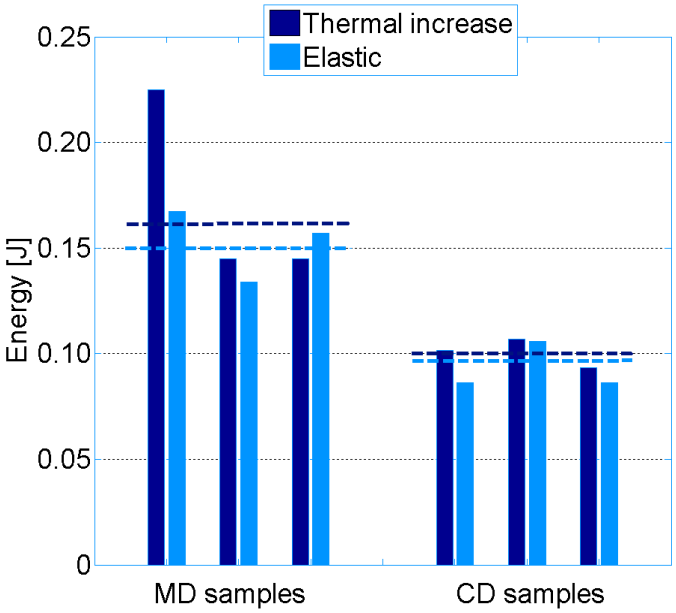

Figure 4.11. Comparison of increase in thermal energy and elastic energy at time of failure for three experiments in MD and CD. Mean values indicated by dashed lines.

Figure 4.11 shows that, apart from one MD sample, the elastic energy and the sudden increase in thermal energy deviated by less than 10%. The result implies that the elastic energy stored in the sample fueled the rupture of the paper samples. This concept has been stated already before [61, 62], however it has not been verified experimentally in thermographic studies on the deformation in paper.

5 Conclusions and future work

5.1 Conclusions

An angle-resolved goniometric method for emittance measurements was developed. The aim was to obtain emittance values for a more accurate use of thermography in the papermaking process, and also for future modelling of the infrared emission from paper at different stages in the papermaking process. The developed method was based on the reference emitter methodology and utilized an infrared camera to measure the emittance. To verify the developed method, systematic tests of different influencing parameters were made and results obtained with the method were compared to emittance values reported in earlier studies by other authors, and also measured with other methods. The emittance dependence on pulp type, pulp drying, refining, fibre orientation, coating, temperature, wavelength range, observation angle, and moisture ratio was investigated.

The emittance of the investigated samples showed a significant dependence on wavelength range, observation angle, and moisture ratio. In all measurements, the LWIR emittance, i.e. in the wavelength range between 7.5 and 13.0 μm, was higher than the MWIR emittance, i.e. in the range between 3.0 and 5.0 μm. For a given wavelength range, the emittance of the different pulp types was similar, with the exception of the thermo-mechanical pulp (TMP). TMP exhibited a significantly lower emittance compared to the other pulp types. Overall, the impact of different sample properties was much smaller in the LWIR range than in the MWIR range. At observation angles larger than 60° from the normal, a marked drop in the MWIR emittance was observed. For the LWIR range, this drop was observed at angles larger than 70°. The emittance of the moist samples increased with increasing moisture ratio. This was expected since the emittance of pure water is higher than that of paper. Here, it was found that the emittance of a moist sample could be approximated by a “mixing rule”, i.e. by a mass-share based linear combination of the emittance of pure water and that of a dry sample.

The application shown in this work clearly illustrated the usefulness of thermography for investigations in the field of pulp and paper. It was found that the observed increase in thermal energy at the time of rupture corresponded well to the value of the elastic energy that had been built up in the sample by tensile forces. Here, the emittance value obtained by the goniometric method increased the accuracy of the thermal energy calculation.

Several implications can be concluded from the results when considering thermography for measurements in the production of paper and board. Cameras operating in the LWIR range appear to be better adapted for measurements in an industrial environment. The emittance of paper and board was highest in the LWIR range. This implies that a measurement in the LWIR range represents a more robust method. When the emittance is high, possible error sources from the surroundings, for example reflections, can only have minor influence on the measured temperature. In addition, LWIR emittance was less sensitive to different paper properties, such as pulp type. This implies a considerable advantage, as several different pulp grades, or pulp mixtures, are used when producing a

certain paper grade. Thus, the risk of emittance-based measurement inaccuracy is reduced. At present, standard LWIR cameras (microbolometers) do not reach the same sensitivity and frame rate as MWIR cameras. However, recent development suggests that the gap between MWIR and LWIR cameras is decreasing [63, 64].

5.2 Suggestions for future work

The emittance values measured in this work can be used to improve the understanding of the infrared emission from paper at different stages in the papermaking process. Additional emittance measurements would be of interest in order to increase the number of quantitative values available. In particular, the emittance of different non-fibre material that are frequently used in paper production (e. g. fillers, brightness additives or coating pigments) need to be added to the present data. Here, the applicability of the mass-share based "mixing rule" to predict the emittance of moist two-ply samples could also be investigated.

The application of quantitative thermography when studying the mechanical deformation of paper gave promising results. Other interesting investigations can be made in this field. For example, an experimental set-up could be used where two mirrors are used to simultaneously image both sides of a sample using thermography. This approach would be of particular interest to study the mechanical behaviour of two-ply samples, where the amount of energy generated at each side could be measured directly when the sample is deformed. Such a study would increase the understanding regarding to what extent the different pulp types in the two plies contribute to the total strength of the sample and interact with each other. Another application of thermography could be the evaluation of packaging structures, for example shopping bags made from paper. Here, due to the possibility of detecting the dissipation of plastic energy already during the deformation of the sample, i.e. before its rupture, weak spots can be identified at an early stage.

In general, all applications where quantitative temperature data from thermography is desired may benefit from accurate emittance values, also taking into account their directional dependence. For example, measured emittance values as a function of moisture ratio could increase the accuracy in reported efforts of using quantitative thermography to infer the moisture distribution of a sheet. Thermography can also be used to measure the temperature of paper during the drying process, for example to quantify drying variations. Differences in drying are known to influence the uniformity in paper properties.

In conclusion, thermography has a significant advantage compared to many other non-destructive monitoring instruments, as it does not require illumination of the web. Once the emittance of the material is determined, no further calibration is required. Given the reduction in cost and improved frame rate and sensitivity of infrared cameras, attempts could be made to integrate 2D thermography with the Quality Control System (QCS) of a paper machine, to analyse and reduce the variability of the process.

References

1. Phillips, L.A. *Using IR to Diagnose Building Conditions*. InfraMation Newsletter, 2003. **4**.
2. Maldague, X.P.V., *Theory and practice of infrared technology for nondestructive testing*. Microwave and optical engineering, ed. K. Chang, 2001, Published by Wiley.
3. Dewitt, D.P. and G.D. Nutter, *Theory and Practice of Radiation Thermometry*. 1st ed, 1988, Published by Wiley-Interscience. New York.
4. Vollmer, M. and K.-P. Möllmann, *Infrared Thermal Imaging: Fundamentals, Research and Applications*. 1st ed, 2010, Published by Wiley-VCH. Weinheim, Germany.
5. McCluney, W.R., *Introduction to Radiometry and Photometry*, 1994, Published by Artech House. Boston.
6. Öhman, C., *Measurement in thermography, ITC Publ. no.: 1 560 055 Rev.A* Infrared Training Center, Stockholm, 2001.
7. Minkina, W. and S. Dudzik, *Infrared Thermography - Errors and Uncertainties*. 1st ed, 2009, Published by John Wiley & Sons Ltd. Chichester, West Sussex, UK.
8. Madding, R.P. *Common misconceptions in infrared thermography condition based maintenance applications*, in Proceedings of *InfraMation 2000*, 2000, Orlando, FL, p. 229-235.
9. NATEC. *Micrographs: Curious collection, teabag*. Internet Microscope for Schools 2012 [cited 2012 2012-10-17]; Available from: http://pwatlas.mt.umist.ac.uk/internetmicroscope/index.html.
10. Mattsson, L. and R. Usbeck. *A technique for analysis of surface and bulk scattering of paper sheets*, in Proceedings of *International Printing and Graphics Arts Conference*, 1996, Minneapolis, p. 131-137.
11. Hainzl, R., et al. *A New Light Scattering Model for Simulating the Interaction Between Light and Paper*, in Proceedings of *TAPPI International Printing & Graphic Arts Conference*, 2002, Savannah, GA, p. 9-17.
12. Banerjee, D., *Development of High Resolution Optical Measurement Techniques to Investigate Moisture Content and Thermal Properties of Paper*, PhD thesis, Fachgebiet Papierfabrikation und Mechanische Verfahrenstechnik, Technische Universität Darmstadt, Darmstadt, 2008.
13. Querry, M.R., B. Curnutte, and D. Williams, *Refractive Index of Water in the Infrared.* Journal of the Optical Society of America, 1969. **59**(10): p. 1299-1306.
14. Penndorf, R., *Tables of the Refractive Index for Standard Air and the Rayleigh Scattering Coefficient for the Spectral Region between 0.2 and 20.0 um and Their Application to Atmospheric Optics.* Journal of the Optical Society of America, 1957. **47**(2): p. 176-182.
15. Jonasz, M. and G. Fournier, *Light Scattering By Particles In Water: Theoretical and Experimental Foundations*. 1st ed, 2007, Published by Elsevier Academic Press. London, UK.
16. Bohren, C.F. and D.R. Huffman, *Absorption and Scattering of Light by Small Particles* 1998, Published by Wiley VCH.
17. Ojala, K.T., E. Koski, and M. Lampinen, *Reflection and transmission measurements with an integrating sphere and Fourier-transform infrared spectrometer.* Applied Optics, 1992. **31**(22): p. 4582-4589.
18. Kokhanovsky, A.A., *Light Scattering Reviews 5: Single Light Scattering and Radiative Transfer*, ed. A.A. Kokhanovsky. Vol. 5, 2010, Published by Springer.
19. Gerber, F., et al., *Modeling directional–hemispherical reflectance and transmittance of fresh and dry leaves from 0.4 μm to 5.7 μm with the PROSPECT-VISIR model.* Remote Sensing of Environment, 2011. **115**(2): p. 404-414.
20. Wang, G., et al., *Design and calculation of low infrared transmittance and emissivity coatings for heat radiative applications.* International Journal of Minerals, Metallurgy and Materials, 2012. **19**(2): p. 179-186.
21. Dolin, L.S. and E.A. Sergeeva, *A model of irradiance distribution for a directed point source in an infiniteweakly absorbing turbid medium.* Radiophys. Quantum Electron., 2001. **44**(11): p. 858–865.
22. Su, R., et al., *Optical coherence tomography for quality assessment of embedded microchannels in alumina ceramic.* Optics Express, 2012. **20**(4): p. 4603–4618.
23. Madding, R.P. *Emissivity measurement and temperature correction accuracy and considerations*, in Proceedings of *SPIE Conference on Thermosense XXI*, 1999, Orlando, FL, p. 393-400.
24. ASTM. *Standard Test Methods for Total Normal Emittance of Surfaces Using Inspection-Meter Techniques*, E408-71, 2008.

25. ASTM. *Standard Test Method for Determination of Emittance of Materials Near Room Temperature Using Portable Emissometers*, C1371-04a, 2004.
26. Puram, C., et al. *Directional Emittance Surface Measurement System and Process*, 1994, US Patent 5.347.128.
27. Beecroft, M., et al. *Hand-held spectrometer*, 2005, US Patent 7.236.243 B2.
28. Bremond, P., et al. *A fast spectral method to measure emissivity in a partially controlled environment using a focal plane array infrared camera*, 2009, US Patent WO2010/089627 A1.
29. Marinetti, S. and P.G. Cesaratto, *Emissivity estimation for accurate quantitative thermography.* NDT&E International, 2012. **51**: p. 127-134.
30. Trepanier, R.J., *The infrared emissivity of wet webs.* Journal of Pulp and Paper Science, 1984(November 1984): p. 166-172.
31. Öhman, C., *Emittansmätningar med AGEMA E-Box, Teknisk rapport*. AGEMA Technical Report (FLIR Systems AB), Stockholm, 1999.
32. Ojala, K., *Studies on infrared drying of paper, use of integrating spheres in FTIR-measurements, and heat and mass transfer inside paper*, PhD thesis, Laboratory of Applied Thermodynamics, University of Helsinki, Espoo, 1993.
33. Griffiths, P. and J.A. De Haseth, *Fourier Transform Infrared Spectrometry*, 1986, Published by Wiley-Interscience.
34. Smith, B.C., *Fundamentals of Fourier Transform Infrared Spectroscopy*. 2nd ed, 2011, Published by CRC Press.
35. Skogsindustrierna. *Energiförbrukning i massa- och pappersindustrin 2011*. [cited 2012 17/10]; Available from: http://www.skogsindustrierna.org/MediaBinaryLoader.axd?MediaArchive_FileID=c1ef257d-8e96-4430-a458-3877e3335dee&FileName=Energienk%C3%A4trapport+2011+DEL_1+text+20120611.pdf.
36. Xia, Q., M. Boyce, and D. Parks, *A constitutive model for the anisotropic elastic–plastic deformation of paper and paperboard.* International Journal of Solids and Structures, 2002. **39**(15): p. 4053–4071.
37. Krook, R., H. Hollmark, and S. Stenström, *Some effects of press drying on paper properties.* Nordic Pulp and Paper Research Journal, 1996. **11**(3): p. 141-151.
38. Gellerstedt, G., *Paper Processes*. The Ljungberg Textbook, 2004, Published by Fibre and Polymer Technology, KTH Royal Institute of Technology. Stockholm.
39. Tysén, A., *In-plane moisture variations and the effects on paper properties and out-of-plane deformation.*, Master thesis, Chemical Engineering, KTH, Stockholm, 2011.
40. Brecht, W., F. Müller, and H. Weiss, *'Uber das 'blasigwerden' von papieren.* Das Papier, 1955. **9**: p. 133-143.
41. Rauhamaa, J. and R. Reinius. *Paper web imaging with advanced defect classification*, in *TAPPI Paper Summit*, 2002, Atlanta, GA, p. 1-12.
42. Rosén, F. and H. Vomhoff. *The use of infrared thermography to detect in-plane moisture variations in paper*, in *Control Systems 2010*, 2010, Stockholm, p. 1-7.
43. Sheahen, T.P., *Use of infra-red thermography in pulp and paper mills.* TAPPI ANNUAL MEETING (Chicago), 1978: p. 173-174.
44. Vickery, D.E., J.E. Luce, and J.W. Atkins. *Infrared thermography - An Aid to solving paper machine moisture profile problems*, in Proceedings of *Tappi Papermakers Conference*, 1978, p. 39-51.
45. Charles, J.A. *Line-scan infrared imaging for papermachine diagnostics*, in Proceedings of *1999 TAPPI Engineering Conference*, 1999, Anaheim, California, p. 9-17.
46. Kiiskinen, H. and P. Pakarinen, *Infrared thermography at examination of paper structure.* Proceedings of SPIE, 1998. **3361**: p. 228-234.
47. Hojjatie, B., J. Abedi, and D.W. Coffin, *Quantitative determination of in-plane moisture distribution in paper by infrared thermography.* Tappi J., 2001. **84**(5): p. 71-82.
48. Dumbleton, D., K. Kringstad, and C. Söremark, *Temperature profiles in paper during straining.* Svensk Papperstid., 1973(14): p. 521-528.
49. Prakash, R.V., *Infrared Thermography*, 2012, Published by InTech. Rijeka, Croatia.
50. Yamauchi, T. and K. Murakami, *Observation of deforming and fracturing processes of paper by using infrared thermography.* Japan Tappi, 1992. **4**: p. 70-75.
51. Tanaka, A. and T. Yamauchi, *Thermographic observations of the out-of-plane tearing process of paper.* Appita Journal, 2005. **58**(3): p. 186-191.
52. Salisbury, J. and D. D'Aria, *Emissivity of Terrestial Materials in the 3-5 um Atmospheric Window.* Remote Sensing of Environment, 1994. **47**: p. 345-361.
53. Rees, W.G. and S.P. James, *Angular variation of the infrared emissivity of ice and water surfaces.*

International Journal of Remote Sensing, 1992. **13**(15): p. 2873-2889.
54. Sobrino, J.A. and J. Cuenca, *Angular variation of thermal infrared emissivity for some natural surfaces from experimental measurements.* Applied Optics, 1999. **38**(18): p. 3931-3937.
55. Niclòs, R., et al., *In Situ angular measurements of thermal infrared sea sirface emissivity -Validation of models.* Remote Sensing of Environment, 2005. **94**: p. 83-93.
56. Hyll, C., H. Vomhoff, and L. Mattsson, *A method for measurement of the directional emissivity of paper; Innventia Report 286*. Innventia Report, Innventia AB, Stockholm, 2011.
57. Lee, H., et al., *Infrared Transmittance of Wet Paper.* Journal of Pulp and Paper Science, 2003. **29**(3): p. 94-98.
58. Smith, C. and J. Wise, *Infrared Spectrometric Examination of Paper. I.* Analytical Chemistry, 1967. **39**(14): p. 1698-1701.
59. Fan, M., D. Dai, and B. Huang, *Fourier Transform Infrared Spectroscopy for Natural Fibres*, in *Fourier Transform - Materials Analysis*, D.S. Salih, Editor 2012, InTech: Rijeka, Croatia. p. 45-67.
60. Mira, M., et al., *Influence of the soil moisture effect on the thermal infrared emissivity.* Tethys, 2007. **4**: p. 3-9.
61. Cavlin, S., *Sprödhetsmodul och kritisk längd (L_krit)*. Teknisk rapport, Svenska Träforskningsinstitutet STFI, Stockholm, 1974.
62. Goldschmidt, J. and D. Wahren, *On the Rupture Mechanism of Paper.* Svensk Papperstid., 1968. **71**(13-14): p. 477-481.
63. Budzier, H., et al., *Fast microbolometer-based infrared camera system*. Publications 20, DIAS Infrared GmbH, Dresden, 2011.
64. Hecht, J., *PHOTONIC FRONTIERS: ROOM-TEMPERATURE IR IMAGING: Microbolometer arrays enable uncooled infrared camera.* Laser Focus World, 2012. **48**(4).

Papers

PAPER A **A METHOD FOR MEASUREMENT OF THE DIRECTIONAL EMITTANCE OF PAPER IN THE INFRARED RANGE**

PAPER B **DIRECTIONAL EMITTANCE OF DRY AND MOIST PAPER**

PAPER C **ANALYSIS OF THE PLASTIC AND ELASTIC ENERGY DURING DEFORMATION AND RUPTURE OF A PAPER SAMPLE USING THERMOGRAPHY**